Sub- and suprathreshold receptive field properties of pyramidal neurones in layers 5A and 5B of rat somatosensory barrel cortex

Ian D. Manns, Bert Sakmann and Michael Brecht

Abteilung Zellphysiologie, Max-Planck Institut für medizinische Forschung, Heidelberg, Germany

Layer 5 (L5) pyramidal neurones constitute a major sub- and intracortical output of the somatosensory cortex. This layer 5 is segregated into layers 5A and 5B which receive and distribute relatively independent afferent and efferent pathways. We performed *in vivo* whole-cell recordings from L5 neurones of the somatosensory (barrel) cortex of urethane-anaesthetized rats (aged 27–31 days). By delivering 6 deg single whisker deflections, whisker pad receptive fields were mapped for 16 L5A and 11 L5B neurones located below the layer 4 whisker-barrels. Average resting membrane potentials were -75.6 ± 1.1 mV, and spontaneous action potential (AP) rates were 0.54 ± 0.14 APs s^{-1}. Principal whisker (PW) evoked responses were similar in L5A and L5B neurones, with an average 5.0 ± 0.6 mV postsynaptic potential (PSP) and 0.12 ± 0.03 APs per stimulus. The layer 5A sub- and suprathreshold receptive fields (RFs) were more confined to the principle whisker than those of layer 5B. The basal dendritic arbors of layer 5A and 5B cells were located below both layer 4 barrels and septa, and the cell bodies were biased towards the barrel walls. Responses in both L5A and L5B developed slowly, with onset latencies of 10.1 ± 0.5 ms and peak latencies of 33.9 ± 3.3 ms. Contralateral multi-whisker stimulation evoked PSPs similar in amplitude to those of PW deflections; whereas, ipsilateral stimulation evoked smaller and longer latency PSPs. We conclude that in L5 a whisker deflection is represented in two ways: focally by L5A pyramids and more diffusely by L5B pyramids as a result of combining different inputs from lemniscal and paralemniscal pathways. The relevant output evoked by a whisker deflection could be the ensemble activity in the anatomically defined cortical modules associated with a single or a few barrel-columns.

Representation of external stimuli in the nervous system is carried out through hierarchical and parallel processes. Despite the extensive work dedicated to this subject, there are relatively few studies which have examined sensory neurones' synaptic input and action potential (AP) output in unison with their specific morphology. The area of somatosensory cortex devoted to the facial whiskers of the rodent, the barrel cortex, possesses an exquisite somatotopy (Woolsey & Van der Loos, 1970). Its layer 4 (L4) neurones, which receive the lion's share of thalamocortical afferents, are conspicuously grouped into discrete 'barrels', easily identified by their staining for the metabolic enzyme cytochrome *c* oxidase (Woolsey & Van der Loos, 1970; Killackey & Ebner, 1973). Dendritic and axonal arbors of L4 spiny cells form a barrel. Discrete barrel-columns representing predominantly one whisker

include the cortex above and below each barrel from the pia to the white matter. As such, a barrel-column's neurones tend to respond preferentially to its principle whisker (PW) (Simons, 1978; Ito, 1981; Armstrong-James & Fox, 1987).

Layer 5 (L5) neurones of the barrel cortex receive a complex set of inputs, which include all cortical layers as well as several subcortical targets, and their axons give rise to widespread projections both intracortically and subcortically (Wise & Jones, 1977; Killackey *et al.* 1989; Bernardo *et al.* 1990*a*,*b*; Koralek *et al.* 1990; Ito, 1992; Hoeflinger *et al.* 1995; Gottlieb & Keller, 1997). L5 somatosensory cortex is a compound structure, consisting of two cytoarchitectonically discrete sublayers: 5A and 5B (Ito, 1992; Hoeflinger *et al.* 1995; Gottlieb & Keller, 1997). These have relatively independent sets of afferent and efferent fibres belonging to the so-called paralemniscal

and lemniscal sensory pathways and are thought to function in a parallel fashion (Ahissar *et al.* 2000). Located immediately inferior to the granular L4, L5A pyramidal neurones receive thalamic input from the medial posterior (POm) nucleus and as such are considered to participate in the paralemniscal sensory pathway. L5A pyramidal neurones in turn project to the caudate nucleus, and several intracortical sites including motor and secondary somatosensory cortex (Koralek *et al.* 1988, 1990; Mercier *et al.* 1990; Lu & Lin, 1993). Located below L5A, the large L5B pyramidal cells receive thalamic input from the main specific sensory relay the ventral posteromedial (VPM) nucleus and as such are considered to function within the lemniscal sensory pathway. These cells give rise to projections to the superior colliculus, pontine nuclei and spinothalamic tract, and to the trigeminal nucleus with collaterals extending intracortically (Wise & Jones, 1977; Koralek *et al.* 1988, 1990; Chmielowska *et al.* 1989; Mercier *et al.* 1990; Lu & Lin, 1993; Deschenes *et al.* 1994). In addition, L5 cells, seemingly in both L5A and L5B, project to the POm nucleus (Veinante *et al.* 2000).

Another fundamental anatomical organizing principle of the cortex is the 'clustering' of L5 apical dendrites with those of layer 2/3 (L2/3) pyramidal neurones (Feldman & Peters, 1974; White & Peters, 1993; Lev & White, 1997). With this organization, small groups of cells are vertically orientated in 'modules.' In the barrel cortex then, two anatomical structures overlap: the barrels of L4 cells and modules of L5 and L2/3 cells (White & Peters, 1993). Little is known about the function of these modules. One possibility is that they functionally bind neurones across different layers; as such this may compliment the L5 neurones' preferential AP response to coincident inputs at apical and basal dendrites (Larkum *et al.* 1999; Larkum & Zhu, 2002).

Although several extracellular unit studies have described the AP firing patterns of L5 neurones in response to sensory stimulation (Simons, 1978; Armstrong-James *et al.* 1992; Ahissar *et al.* 2000, 2001); only one study has examined L5B cells' receptive field (RF) structure in association with their morphology (Ito, 1992). Despite this, how the RF structure and related cell morphology of L5A is manifest in relation to L5B remains unclear. In the present study, we explored the relationship between sub- and suprathreshold RF properties of L5 neurones, their dendritic and axon arbor morphology, their position in relation to the cytoarchitechtonically defined barrel-column and their potential contribution to cortical modules.

Methods

The techniques employed here have been described in previous studies from this laboratory (Brecht & Sakmann, 2002*a,b*; Margrie *et al.* 2002).

Animals

In each of 45 Wistar rats, aged 26–31 days, one neurone was recorded; however, not all of these cells were recovered, and several recovered cells were not located in L5 of the barrel cortex. In one animal, two cells were recorded with differing cortical depths, both of which were subsequently recovered and thus included in the data set.

Preparation

Experimental procedures were carried out in accordance with the animal welfare guidelines of the Max-Planck-Society. Rats were anaesthetized with urethane (1–1.4 g kg^{-1}; intraperitoneal injection). Access to the barrel cortex was gained by opening a hole in the cranium ~1 mm diameter, posterior 2.5 mm and lateral 5.5 mm from bregma. A small hole in the dura was opened and bathed in Hepes-buffered artificial cerebrospinal fluid (ACSF) solution for subsequent electrode penetration. The depth of anaesthesia was monitored throughout the experiment by assessing hindlimb pinch withdrawal, eyelid reflex, respiration, and vibrissae movements. If vibrissae movements and withdrawal reflexes occurred, additional doses of urethane (20% of initial dose) were given. The respiration rate was between 70 and 100 breaths min^{-1}. Taken together, we considered the depth of anaesthesia to approximate anaesthetic state III-3 (Friedberg *et al.* 1999).

Whole-cell recording

Recordings were made with long tapered 4−7 MΩ resistance patch pipettes pulled from borosilicate glass tubing in a four stage pull. Pipettes were filled with 130 mM potassium gluconate, 10 mM sodium gluconate, 10 mM Hepes, 10 mM phosphocreatine, 4 mM MgATP, 2 mM Na$_2$ATP, 0.3 mM GTP, 4 mM NaCl and 0.4% biocytin at pH 7.2.

Pipettes were lowered perpendicularly to the cortical surface and 1000–1500 μm into the barrel cortex in order to target L5 neurones. To avoid tissue and debris blocking the pipette, it was pressurized to 200−300 mbar during the penetration. To establish the whole-cell recording configuration we used conventional voltage

clamp (Blanton *et al.* 1989; Margrie *et al.* 2002). Series resistances were between 10 and 70 MΩ. All data have been corrected for a +7 mV junction potential.

Sensory stimulation and receptive-field maps

Two principle methods of sensory stimulation were employed. The first of these was single whisker stimulation using a piezoelectric bimorph wafer with an attached glass capillary (Simons, 1983). Steps elicited by the piezoelectric device had a 10–90% rise time of 1 ms. The deflection point of the whisker was chosen to be 8–10 mm from the base of the vibrissa (roughly 6 deg deflection angle) for 200 ms. Care was taken as not to deflect more than one whisker or to cause displacement of neighbouring whisker follicles. Stimuli were delivered at a rate of 1 Hz. The second stimulus was multi-whisker stimulation delivered by an air puff (100 ms), which deflected four to eight whiskers in two to three whisker rows by up to 2 mm.

Data analysis

The postsynaptic potential (PSP) response was taken to be the largest membrane depolarization or hyperpolarization during the initial 100 ms following stimulus onset in averaged traces. The AP count during the 100 ms following stimulus onset was classified as the neurone's suprathreshold response. For PSP latency measurements we determined the time point after whisker deflection onset where the postsynaptic potential reached 5% of its peak amplitude. The directional tuning of the response was quantified by the following equation: (Response in preferred direction − response in opposite direction)/(Response in preferred direction + response in opposite direction). As such, a value of 1 indicates a completely directional response, and zero represents responses without direction preference. Averages are presented throughout followed by ± S.E.M.

Histological procedures and reconstruction

Following the recording, the animals were killed by transcardial perfusion of 4% paraformaldehyde, and their brains were removed. Brains were sectioned in 80 μm or 150 μm sections in either tangential or coronal planes of orientation. Approximately, half of the brains were cut in each orientation. The tangential sections were cut parallel to the surface of the barrel cortex. The coronal sections were cut 45 deg towards the sagittal plane with the medial border being anterior and the lateral border being posterior. This angled-coronal cut was selected to result in sections perpendicular to the barrel

rows and parallel to the barrel arcs. Cytochrome oxidase staining (Wong-Riley, 1979) was used to visualize the cortical layering and barrel structure. The recorded cells were revealed with the chromogen 3,3′-diaminobenzidine tetrahydrochloride (DAB) using the avidin–biotin–peroxidase method (Horikawa & Armstrong, 1988). Processed sections were then mounted on slides and coverslipped with moviol.

Subpial depth and laminar distribution of cells

The brown appearance of L4 due to the cytochrome *c* stain combined with the relatively chromogen-free appearance of L5A provided a very clear demarcation of the L4/L5A border. From histological examination this border occurred in our sections at an average depth of ∼975 μm. The L5A/L5B border was marked by a gradual increase in brown cytochrome *c* stain, cell density and the appearance of larger cells. This transition from L5A to L5B generally occurred at an average of ∼310 μm below the L4/L5A border. The L5B/L6 border was indicated by a relatively chromogen-free stripe between the darker stained L5B and upper layer 6 (L6); this generally occurred at ∼1575 μm.

Plots of RFs and of dendritic and axonal densities

Smoothed RF plots were generated by linear interpolation. The conversion of reconstructed neurones to 2-D density maps was done according to the method of Brecht & Sakmann (2002*a*). In brief, to generate 2-D maps of dendritic and axonal densities, the total length of all dendrites or axons within 50 μm voxels was calculated. The resulting 3-D matrix was projected onto either a tangential or coronal plane resulting in a 2-D density matrix. This 2-D density matrix was then low-pass filtered by convolving it with a 2-D Gaussian kernel with a standard deviation of 50 μm. A bicubic interpolation of the filtered 2-D density matrix was preformed to generate the 2-D density map. For averaging dendritic and axonal arborizations across cells, the reconstructions were aligned relative to the centre of the respective barrel.

Results

We examined the RF properties of 27 L5 pyramidal cells of the barrel cortex by whole-cell recordings and subsequent anatomical reconstructions. In response to depolarizing current injection, L5 neurones responded with either regular ($n = 14$) or burst ($n = 13$) firing patterns. The membrane potential (V_m) in all cells showed spontaneous depolarizations between ∼10 and 15 mV (up-state) from

Table 1. Passive membrane properties of layer 5 cells

	All cells ($n = 27$)	Layer 5A ($n = 16$)	Layer 5B ($n = 11$)
RP (mV)	-75.6 ± 1.1	-77.5 ± 1.4	-74.4 ± 1.8
Steady state R_{in}	44.2 ± 4.7	45.3 ± 6.0	42.6 ± 8.1
Depolarization required for AP initiation (mV)	20.9 ± 0.9	21.0 ± 1.4	20.6 ± 1.0
Spontaneous AP activity (APs s^{-1})	0.54 ± 0.14	0.39 ± 0.14	0.77 ± 0.28

RP refers to the initial resting membrane potential. The value reported refers to that taken during the hyperpolarized period (down-state) between ongoing spontaneous depolarizations (up-states). The R_{in} was calculated by injecting -100pA into the soma and determining the voltage drop 300 ms after current-injection onset.

Table 2. Morphometric characteristics of layer 5 cells

	All cells	Layer 5A	Layer 5B
No. of cells	27	16	11
Soma diameter (μm)	17.1 ± 0.7	16.8 ± 0.9	17.73 ± 1.2
Soma area (μm^2)	237.7 ± 12.1	236.4 ± 16.6	239.9 ± 30.9
No. of dendrites	6.2 ± 0.5	6.6 ± 0.6	5.4 ± 0.6
Total dendritic length (μm)	7614.1 ± 765.9	7454.8 ± 773.4	7853.1 ± 1582.8
Horizontal dendritic field span (μm)	333.6 ± 30.5	346.9 ± 46.9	317.5 ± 40.8
Vertical dendritic field span (μm)	1082.3 ± 57.2	1000.6 ± 51.5	1327.7 ± 73.0

No. of dendrites refers to primary basal dendrites.

a relatively flat resting state (down-state), which was taken to be the resting membrane potential (Table 1). These membrane potential fluctuations are similar to those previously described in cortical neurones (Cowan & Wilson, 1994; Anderson *et al.* 2000; Sachdev & Wilson, 2001; Petersen *et al.* 2003). Associated with this ongoing subthreshold activity, these cells often fired spontaneous action potentials (APs), on average ∼0.5 APs s^{-1} (Table 1).

Reconstruction of the recorded neurones revealed these L5 pyramidal neurones to possess an average of approximately six basal dendrites (Table 2) and a long branching apical dendrite sparsely populated with spines. Dendrites and axonal arbors were reconstructed in relation to the cytoarchitechtonic boundaries of the barrel cortex with specific care taken to delineate layer and the whisker-barrel boundaries (Figs 1 and 2). This being done, they were found distributed below the whisker-barrels domain of L4, throughout L5A and L5B with 16 and 11 neurones in each layer, respectively. The majority were located throughout rows E and C between arcs 1 and 4.

RF structure, morphology and barrel-column position

L5 cells responded to deflection of single whiskers with depolarization of the membrane potential, taken to be postsynaptic potentials (PSPs), and less frequently APs (Figs 1*B* and 2*B*). The principle whisker (PW), in our case taken to be the whisker evoking the greatest PSP, was determined by systematically deflecting different whiskers

(Figs 1 and 2). As illustrated for a L5A neurone in Fig. 1, D2 whisker deflections evoked the largest PSPs, making it the PW, while the next largest PSPs were evoked by the D3 surround whisker (SuW). This L5A cell's RF was relatively sharply tuned, the D3 SuW average PSPs represent less than half the amplitude of the PW, and many whiskers did not evoke detectable PSPs (Fig. 1*C*). Although the number of APs evoked by whisker stimulation was low, it was greatest again for the PSP-derived PW, D2 (Fig. 1*C*). PSP size did not necessarily correspond perfectly with number of evoked APs. This is evident for this cell's SuWs. The D3 whisker evoked larger PSPs than the D1; however, the D1 whisker evoked more APs than the D3 whisker due to ongoing spontaneous up- and down-state related AP activity. The anatomical location of this neurone within the D2 barrel (Fig. 1*A*) demonstrates correspondence between the physiologically derived PW and the cell's anatomical location in the PW barrel-column. This cell's morphology is typical of L5A pyramidal neurones, with several basal dendrites, an apical dendrite with a tuft in layers 1 and 2, and an axon which projects to the white matter as well as bifurcating and projecting intracortically within and beyond the barrel cortex. Figure 2 illustrates the RF properties of a L5B neurone. The E2 PW PSPs for this cell are only marginally larger than the responses of the D2 and E3 SuWs. All whiskers deflected evoked both PSP and AP responses. The anatomical location corresponds to its PSP-derived PW; however, the number of evoked APs was greater for SuWs, reflecting the interaction
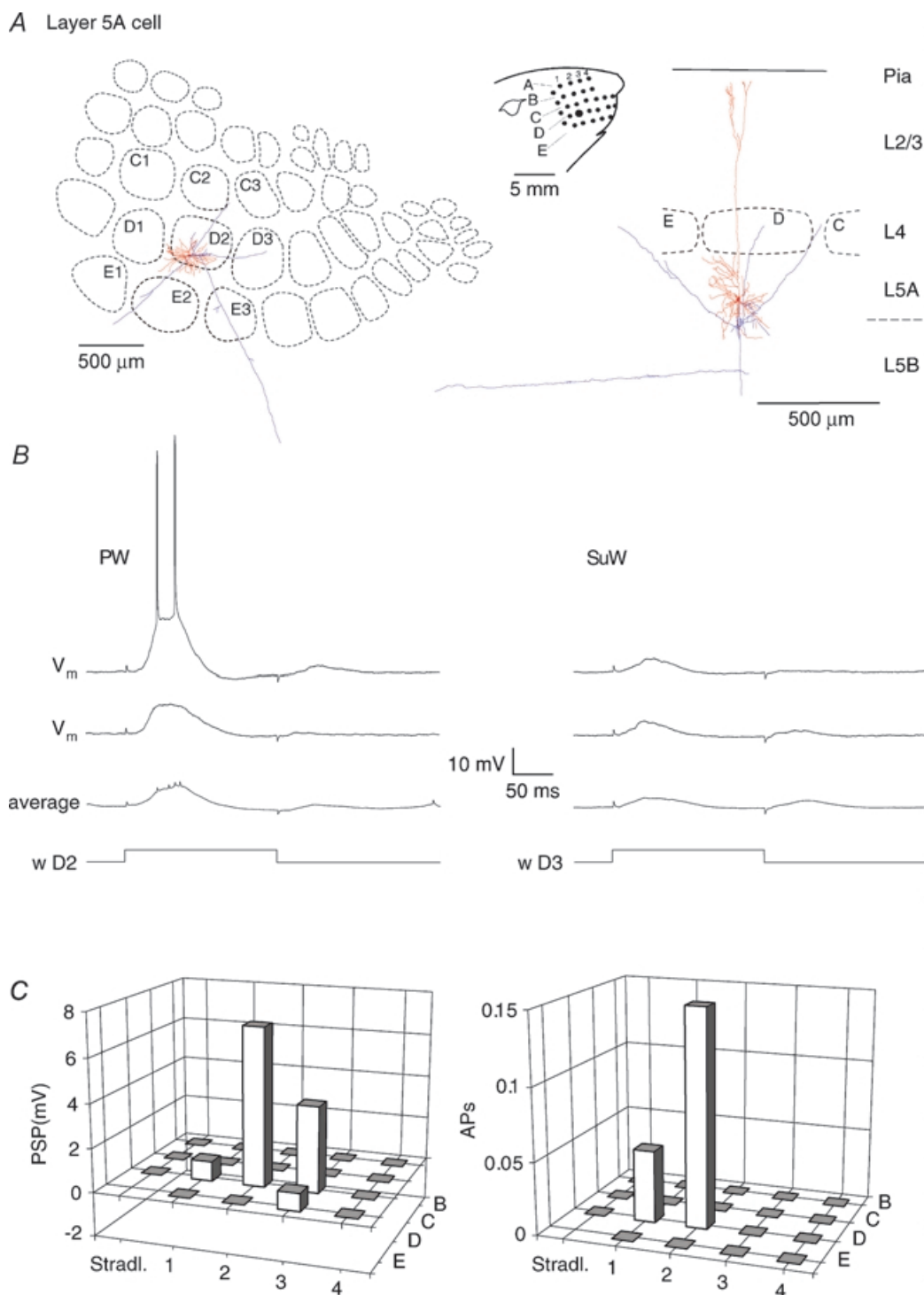
Figure 1. Sensory responses and anatomy of a layer 5A (L5A) somatosensory pyramidal neurone
A, the rat's whisker pad, represented in the centre, provides reference for the whiskers' corresponding cortical barrels shown in the left and right panels. Dendritic (red) and axonal (blue) arborizations of the recorded neurone across the barrel cortex viewed from tangential (centre) and coronal (right) perspectives. From the coronal view, the cell body resides in L5A. *B*, whisker stimulation (w) evoked membrane potential (V_m) responses in D2 principle (PW) and D3 surround whiskers (SuW). The average membrane potential responses are shown in the lower traces. The time course of the whisker deflection is shown below the averages. *C*, subthreshold (left) and suprathreshold (right) receptive fields (RFs). The height of each bar represents the average postsynaptic potential (PSP) or number of action potentials (APs) evoked by each stimulus for the respective whiskers of the whisker pad (Stradl. refers to the straddler whiskers).
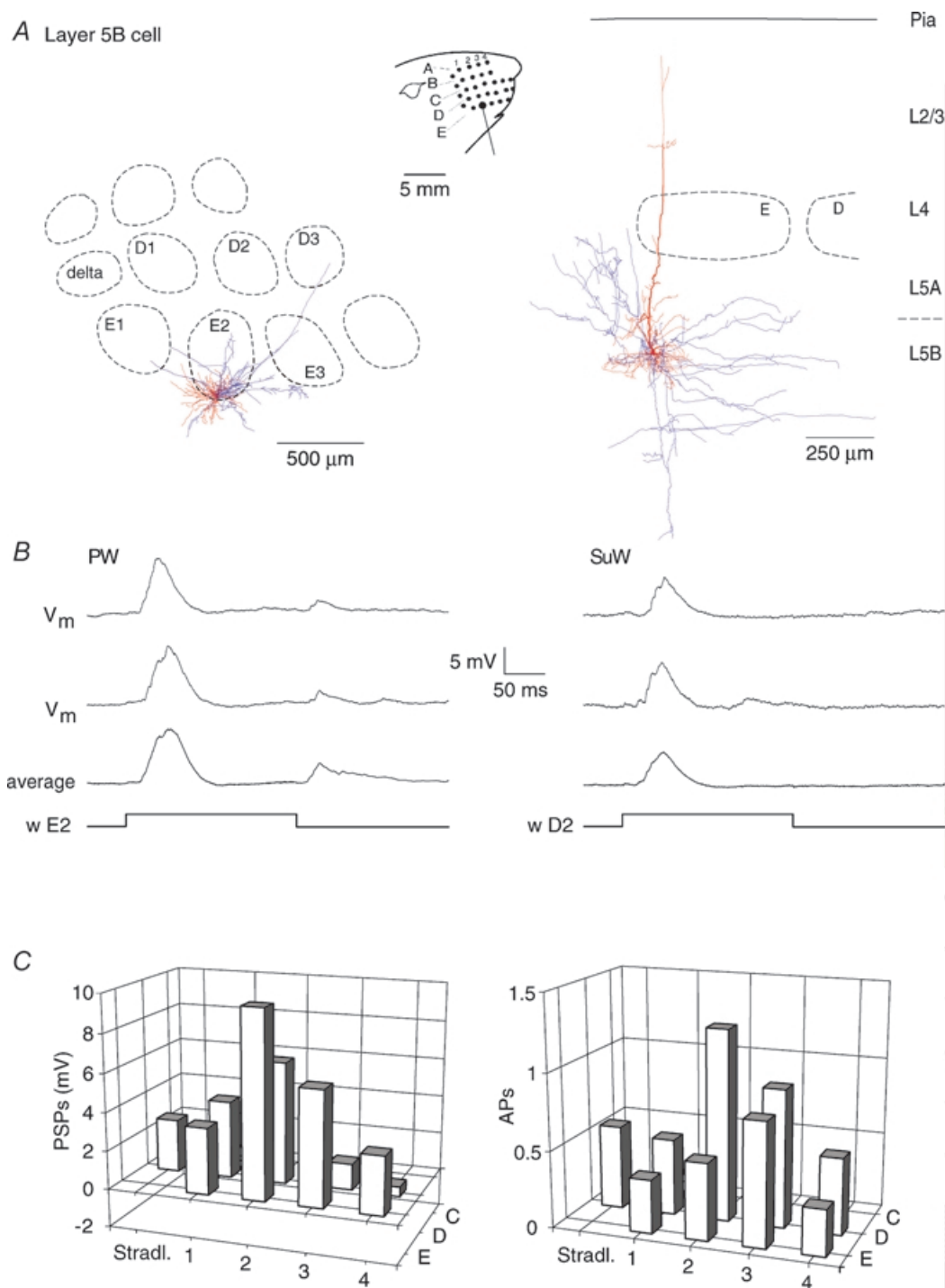
Figure 2. Sensory responses and anatomy of a L5B somatosensory pyramidal neurone
A, the rat's whisker pad, represented in the centre, provides reference for the whiskers' corresponding cortical barrels shown in the left and right panels. Dendritic (red) and axonal (blue) arborizations of the recorded neurone across the barrel cortex viewed from tangential (centre) and coronal (right) perspectives. From the coronal view, the cell body resides in L5B. *B*, whisker stimulation (w) evoked membrane potential (V_m) responses in E2 principle (PW) and D2 surround whiskers (SuW). The average membrane potential responses are shown in the lower traces. The time course of the whisker deflection is shown below the averages. *C*, subthreshold (left) and suprathreshold (right) receptive fields (RFs). The height of each bar represents the average postsynaptic potential (PSP) or number of action potentials (APs) evoked by each stimulus for the respective whiskers of the whisker pad (Stradl. refers to the straddler whiskers).

between evoked PSPs and spontaneous APs occurring as a function of the up- and down-states. This cell's anatomy is common among the large L5B pyramidal neurones, with many dendrites extending beyond the home-barrel column, a relatively thick apical dendrite, and axonal arbors projecting towards the white matter as well as within the barrel cortex.

The neurones' physiologically derived PW corresponded to their anatomical whisker-barrel location in all tangential sections with unequivocal cytochrome *c* barrel staining ($n = 10$). We did not identify any of our cells as having their cell body in the L5 septal-related region. To further compare the RF properties of the L5 cells with their anatomical geometries (Table 2), we calculated normalized population RFs and constructed 2-D maps of the average dendritic and axonal densities of our corresponding reconstructed cells in each layer. Tangential reconstructions (L5A: $n = 6$; L5B: $n = 4$) were rotated into the coronal orientation to be used in the construction of coronal density maps, whereas coronal reconstructions could not be accurately rotated into the tangential position since barrel borders could not be reliably determined within the rows (e.g. a D1 to D2 barrel/septum/barrel transition would be difficult to determine across sections).

In Fig. 3*A*1 and *A*2, the average normalized sub- and suprathreshold L5A RFs, with a superimposed barrel pattern, allow visualization of the discrete PW-evoked PSPs and APs, in addition to the sharp fall-off in SuW-evoked PSPs and APs. Visualized in the 2-D density plots (Fig. 3*B* and *D*), the dendritic arborizations compliment the RF excitation pattern by extending throughout the home barrel-column. Most of the dendritic density is confined to L5A. Some dendritic arbors extend laterally into the septa as well as vertically into the other layers. The apical dendrites and their arborizations contribute to the vertical spread into L4 and the prominent tuft in L2/3 and L1. The 2-D projection map of the L5A axonal arbors (Fig. 3*C* and *E*) illustrates that the axonal projection extends both laterally throughout L5A and vertically into the superior and inferior layers towards the white matter.

In Fig. 4*A*1 and *A*2, the average normalized sub- and suprathreshold L5B RF allows visualization of a broad, in comparison to L5A, excitation of evoked PSPs and APs by both PW and neighbouring SuWs. The dendritic arborizations (Fig. 4*B* and *D*) compliment the RF excitation pattern; the dendrites extend not only through the home barrel but spread horizontally across the septa and into neighbouring barrels. Most of the dendritic density is within L5B, yet the dendritic arbors extend laterally into the septa and neighbouring barrels and

vertically into the other layers. The L5B apical dendrites and their arborizations contribute to spread of dendrites in L5A and L4 and the prominent tuft in L2/3 and L1. The axonal arbors appear largely confined to L5B with lateral as well as descending and ascending projections (Fig. 4*C* and *E*).

Figure 5 shows a representation of all L5 cells recovered from tangential sections superimposed on an idealized home-barrel. Although we did not identify any of our cells as having their cell body in the septal region, the preference of our recorded cells to hug the barrel/septum border and to extend their dendrites into and across septa is obvious (Fig. 5). When the barrels were subdivided into three concentric zones of equal area, 40% of cells were in the outer most area, while 30% resided in the middle area and another 30% in the inner area. From the tangential reconstructions, the average distance of L5A and L5B cells to the barrel border was $16 \pm 3\%$ and $11 \pm 6\%$ of the home-barrel cross-sectional diameter. As a percentage of all the cells reconstructed from both tangential and coronal sections, 87% of L5A and 80% of L5B cells sent dendritic arbors into the septa, while 46% and 60% of these cells sent arbors into neighbouring barrels. The number of basal dendritic arbors extending into neighbouring barrels was 1.9 ± 0.6 for L5A cells and 3.7 ± 1.7 for L5B cells. However in coronal reconstructions, it was difficult to visualize dendritic spread across the barrel rows, so the former numbers should be treated as estimates.

In general, L5A neurones responded with PSPs to fewer whiskers than L5B neurones, 5.4 ± 0.8 and 8.0 ± 0.9 whiskers, respectively ($t = 2.1$, d.f. $= 25$, $P = 0.048$). The average population subthreshold and suprathreshold RFs for L5A and L5B were qualitatively different, with that of L5A having a sharper drop in average evoked PSP amplitude or average evoked APs from the PW to the SuWs (Figs 3*A*, 4*A*, and 6). This sharpness or acuity was evaluated by calculating the decrease in average values from the PW to those of the average primary surround whisker (Su1W) and secondary surround whisker (Su2W) responses – all the first neighbour and second neighbour whiskers, respectively. In terms of PSPs, the L5A cells' Su1W and Su2W average amplitudes fell, respectively, to 27.0 ± 6.0 and $3.7 \pm 1.3\%$ of the PW amplitude, while those of the L5B cells fell to $41.9.6 \pm 7.7$ and $17.7 \pm 7.6\%$. The acuity, measured by the slope of the regression line for each cell's normalized PW, Su1W and Su2W values, was steeper for the L5A neurones than for those of L5B ($t = 2.2$, d.f. $= 25$, $P = 0.04$). In terms of APs, the L5A cells' Su1W and Su2W average values fell, respectively, to 20.4 ± 6.9 and $8.7 \pm 6.8\%$ of the PW value, while those of the 5B cells fell to 63.9 ± 16.0 and $48.3 \pm 21.5\%$. In the cells that
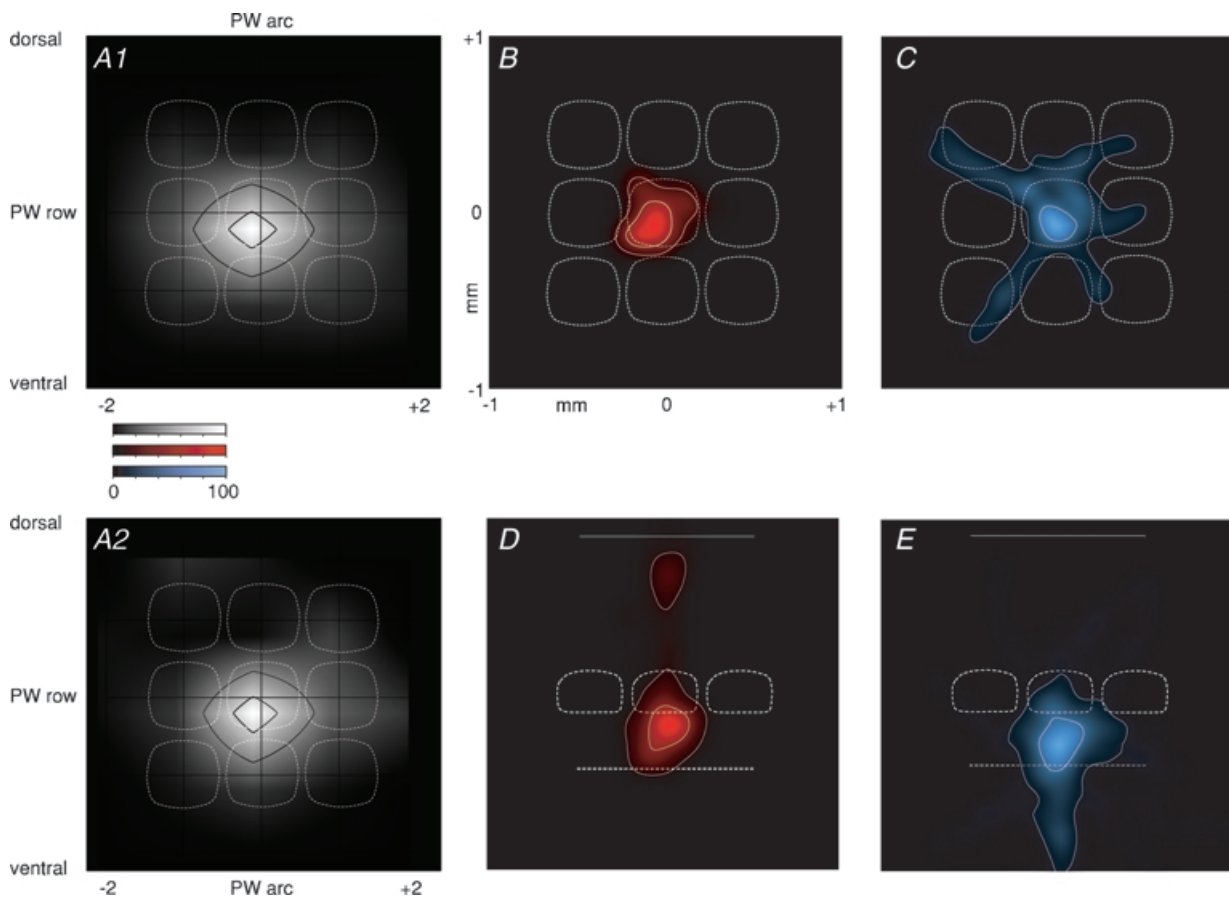
Figure 3. Subthreshold RF map and dendritic and axonal segment density plots of L5A neurones
*A*1, average normalized subthreshold RF map for L5A cells (*n* = 15); note that it is offset to match the area of maximal dendritic density in *B*. The black grid indicates whisker positions, given with respect to the PW. Whisker positions are given by intersection of horizontal and vertical lines. The ordinate −2 refers to the caudally located SuWs in the second arc posterior to the PW. Similarly, the ordinate +2 refers to the rostrally located SuWs in the second arc anterior to the PW. On the abscissa 'dorsal' indicates whisker positions above the PW, and 'ventral' whisker positions below the PW. The response amplitude is indicated by the brightness normalized to the peak of the PW deflection amplitude determined in each experiment. The black contour line delineates an area on the RF map responding with ∼50% of the PW peak response amplitude. An average cytoarchitectonic L4 barrel field pattern (white, dashed lines) in the horizontal plane is superimposed for comparison of the average RF structure. Outlines above the PW barrel correspond to barrels located laterally. Outlines to the right of PW barrel outline correspond to barrels located anterior to the PW barrel. *A*2, average normalized suprathreshold RF map for L5A cells. The conventions are the same as in *A*1. *B*, average 2-D map of dendritic length density (red, *n* = 6) projected on to the tangential horizontal plane. The average barrel field is superimposed (white, dashed lines) for comparison as in *A*. The inner white contour line delineates an area that contains densities that are ∼50% of the maximal density of dendrite segments. The outer white contour line delineates an area that includes 80% of all dendrite segments. *C*, average 2-D map of axon 'length density' (blue, *n* = 6) projected on to the tangential horizontal plane as in *B*. *D*, average 2-D map of dendritic length density (red, *n* = 16) projected on to the coronal vertical plane along the barrel arcs. The dashed lines represent outlines of averaged barrels: centre, PW barrel; right, lateral barrel; left, medial barrel. The dashed line below the barrels demarcates the L5A/L5B transition, while the continuous white line above represents the cortical surface. The contours are the ∼50% maximal density, and 80% of all segments as in *B*. *E*, average 2-D map of axon length density (blue, *n* = 15). Projection onto the coronal vertical plane as in *D*.

had evoked APs, the population AP RF acuity was again higher for L5A than L5B ($t = 2.7$, d.f. = 15, $P = 0.02$).

In one experiment, two neurones were sequentially recorded and labelled, one in L5A and one in L5B. These cells were found to be within the same putative 'cortical module' or 'cluster' (Fig. 7*A*). Following the typical pattern, the L5A cell has a relatively narrow RF in comparison to the L5B cell (Fig. 7*B*). The apical dendrites of the two cells come in very close proximity within L4, similar to what has been reported for L5 apical dendrites of cortical modules (White & Peters, 1993). This suggests that from single cortical modules different layer-specific information, in this case from L5A and L5B, is sent to target neurones. The axons of these cells were traced

to several putative target sites. The L5A cell projected intracortically to secondary somatosensory cortex, and its main axon entering the corpus callosum branched with one branch extending across the midline while the other branch projected to the caudate nucleus ipsilaterally. The L5B cell sent its main axon into the corpus callosum; it then continued ipsilaterally into the cortical peduncle heading towards the brainstem.

The PW-PSPs of L5A and L5B cells had similar properties (Table 3). The average onset time of L5A cells lagged that of L5B cells, but the times were not significantly different. For L5 cells in general, the average latencies to PSP onset and peak became slightly longer on changing stimulation from the PW (onset, 10.1 ± 0.5 ms; peak,
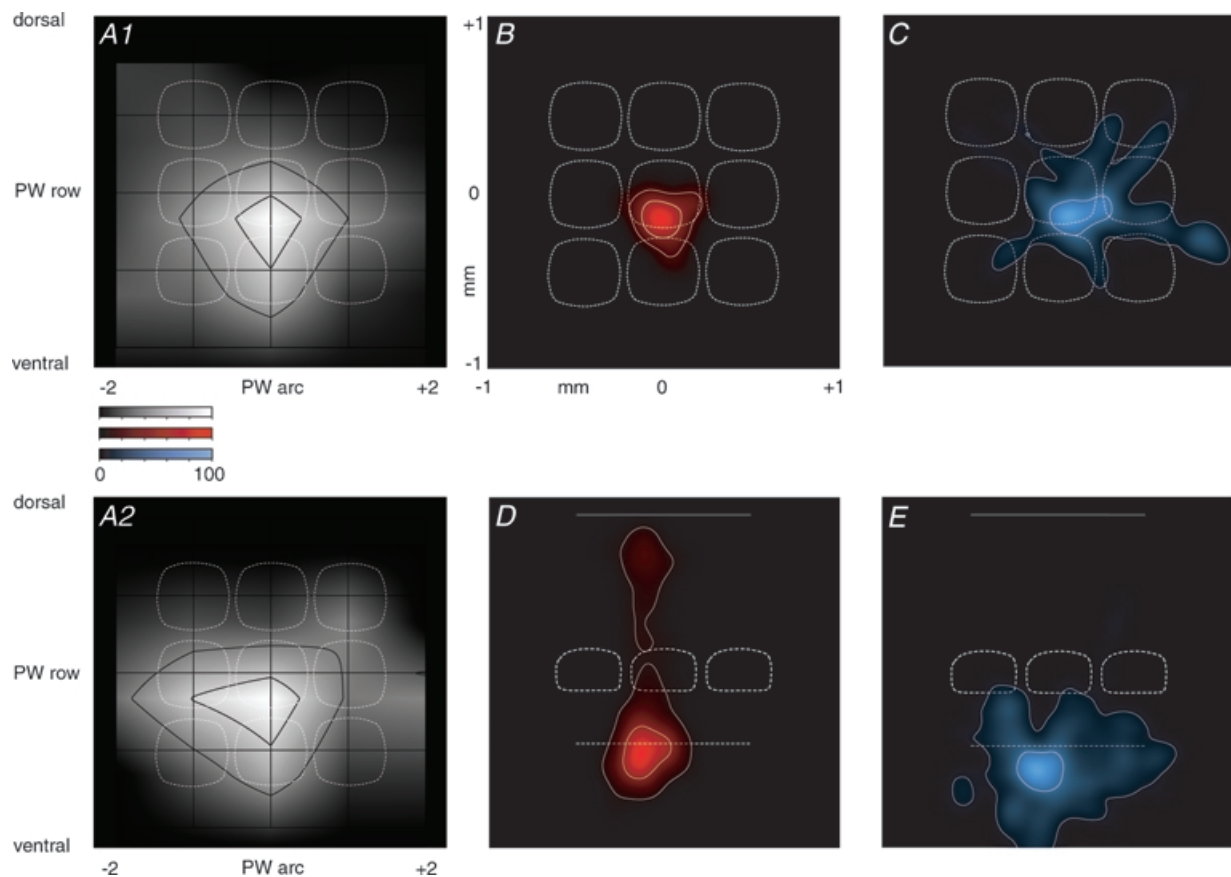

Figure 4. Subthreshold RF map and dendritic and axonal segment density plots of L5B neurones
*A*1, average normalized subthreshold RF map for L5B cells (*n* = 11). All conventions are the same as for Fig. 3*A*. *A*2, average normalized suprathreshold RF map for L5B cells. The conventions are the same as for Fig. 3*A*1. *B*, average 2-D map of dendritic length density (red, *n* = 4) projected on to the tangential horizontal plane; conventions as for Fig. 3*B*. *C*, average 2-D map of axon 'length density' (blue, *n* = 4) projected on to the tangential horizontal plane as in *B*. *D*, average 2-D map of dendritic length density (red, *n* = 11) projected on to the coronal vertical plane along the barrel arcs; conventions as for Fig. 3*D*. *E*, average 2-D map of axon length density (blue, *n* = 11). Projection on to the coronal vertical plane as in *D*.

33.9 ± 3.3 ms) to the Su1Ws (11.6 ± 0.4 ms; 37.3 ± 2.7 ms) and then to the Su2Ws (13.6 ± 1.5 ms; 44.7 ± 6.4 ms; Table 3). The population-average PSPs for PWs and all Su1Ws and Su2Ws are compared for L5A and L5B cells in Fig. 8. The PW PSP time course of L5A cells (11.2 ± 2.1 ms 20–80% rise time; 35.1 ± 3.7 ms peak latency; decay time constant 51.9 ± 6.0 ms) was very similar to that of the L5B cells (7.8 ± 1.1 ms 20–80% rise time; 32.2 ± 2.2 ms peak latency; decay time constant 52 ± 8.6 ms). Whisker responses were obviously dominated by EPSPs masking potential inhibitory PSPs (IPSPs). Although we did not systematically examine the potential contribution of IPSPs to responses by changing the membrane potential, we did notice that hyperpolarization often followed the initial PW-evoked EPSP in L5A cells ($n = 10$; 63% of cells); this was less common among L5B cells ($n = 4$; 36% of cells).

To visualize the dynamics of the PSPs across the RF, we calculated averaged normalized population PSPs for PWs,
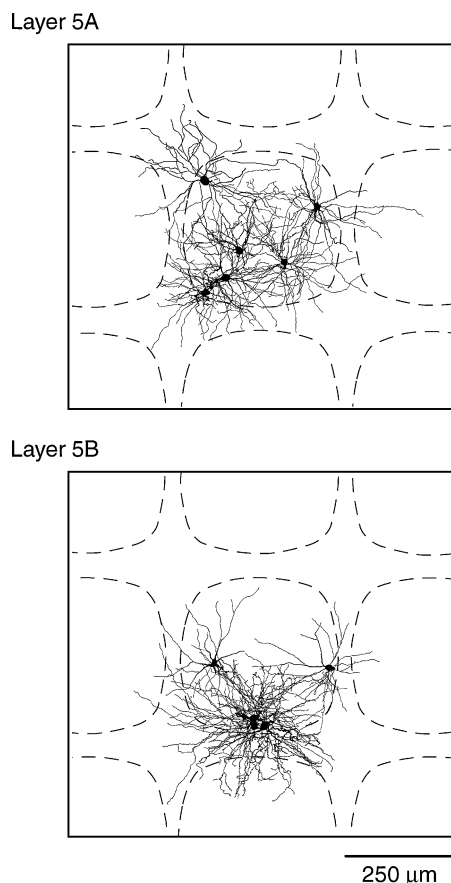
Layer 5A

Layer 5B

250 μm

Figure 5. Distribution L5A ($n = 6$) and L5B ($n = 4$) reconstructed cells from tangential sections superimposed on an idealized barrel

Whisker-barrel conventions the same as Fig. 4. Note the positioning of most cells proximal to the barrel/septum border and the extension of dendrites into septa and neighbouring barrels.

Su1Ws and Su2Ws at discrete time points following the stimulus presentation (Fig. 9). It is evident that excitation is dominant for the PW in the 40 ms time window following the stimulus onset; while by 160 ms, the signal has faded. In the L5A cells, SuWs contribute little overall signal. While in the L5B cells, they contribute relatively more or less during different periods of the response. In general, the L5A RFs are considerably more restricted in the horizontal plane to the PW than are those of L5B.

Figure 10 illustrates neuronal firing in response to PW deflections. Of the L5A and L5B cells 10 and 6, respectively, increased their AP firing in response to the PW deflections, while many other neurones did not increase their AP discharge in response to the stimulation (Fig. 10). Of those that did increase their AP firing, 8 of the 10 L5A and 4 of the 6 LB cells increased their rate of firing at least 2-fold. The evoked activities in L5A and L5B cells were 0.12 ± 0.03 and 0.13 ± 0.05 APs per stimulus, respectively, and were not significantly different. This L5 evoked activity was significantly greater than spontaneous activity (paired *t* test, $t = 3.37$, d.f. = 26, $P < 0.002$), with the spontaneous activity representing on average 31.3 ± 5.5% of the evoked activity. The latencies to maximal discharge of L5A and L5B cells were 39.2 ± 7.4 ms and 48.7 ± 7.9 ms, as measured, when possible, from individual cell peristimulus histograms (Fig. 10).

Variation of stimulus parameters

Different stimuli were used to explore the responsiveness of the L5 neurones.

The directionality of the neurones was tested by deflecting the PW in four different directions (Fig. 11). Figure 11*A* shows a cell that responds with larger amplitude responses in the forward direction. Both L5A and L5B neurones showed similar directionality preferences with the amplitude of the preferred direction being ~40% greater than that of the opposite direction, given by the directionality index (Fig. 11*C*). One direction always responded best, and for 50% of neurones, this was the backward direction (Fig. 11*D*). In the cells tested, the best-direction average PSP amplitude was 4.6 ± 0.8 mV; this was significantly greater than the PSP amplitude caused by backward deflection 3.8 ± 0.7 mV ($t = 2.4$, d.f. = 15, $P = 0.03$). However, the best-direction average evoked AP activity was 0.11 ± 0.05 APs per stimulus, not greater than that evoked by backward deflection 0.10 ± 0.05 APs per stimulus.

To determine the response pattern of L5 neurones to repetitive stimuli, we stimulated the PW at 10 Hz. Figure 12 illustrates the average responses in a subset of L5A and L5B

cells. The successive PSPs rapidly declined in amplitude in both L5A and L5B cells such that by the third stimulus the evoked responses were equal to 30% of the initial response (Fig. 12*C*). The L5A cells occasionally showed sustained depolarization to the 10 Hz stimulation (4 of 9 cells; Fig. 12).

When multiple whiskers were stimulated on the contralateral whisker-pad (deflection of 4–8 whiskers by ∼10 deg) as opposed to simply the PW there was an insignificant increase in the evoked PSP and APs in both L5A and L5B (Fig. 13). In cells where both measures were taken, the L5A cells ($n = 16$) average multi-whisker response was ∼1.4 mV greater than that of the PW response, while in L5B cells ($n = 9$) it was ∼1.2 mV

larger. As such, the L5 multi-whisker evoked PSP was 6.3 ± 0.9 mV with a corresponding 0.19 ± 0.10 APs per stimulus.

When multiple whiskers were stimulated on the ipsilateral whisker pad, we found PSPs in the majority of cells (66%; $n = 6/9$), with no difference between L5A (1.4 ± 0.8 mV; $n = 3$) and L5B cells (3.7 ± 1.9 mV; $n = 3$). Compared to PSPs evoked by contralateral stimulation, the ipsilaterally evoked PSPs lagged their contralateral counterparts' average onset by 22.6 ± 5.2 ms. The ipsilateral response size varied from cell to cell (range = 0.4–6.9 mV), but they were consistently smaller than the contralateral peak amplitude by $34.9 \pm 8.0\%$ ($t = 2.4$, d.f. = 4, $P = 0.03$). Figure 14 shows average ipsilateral and
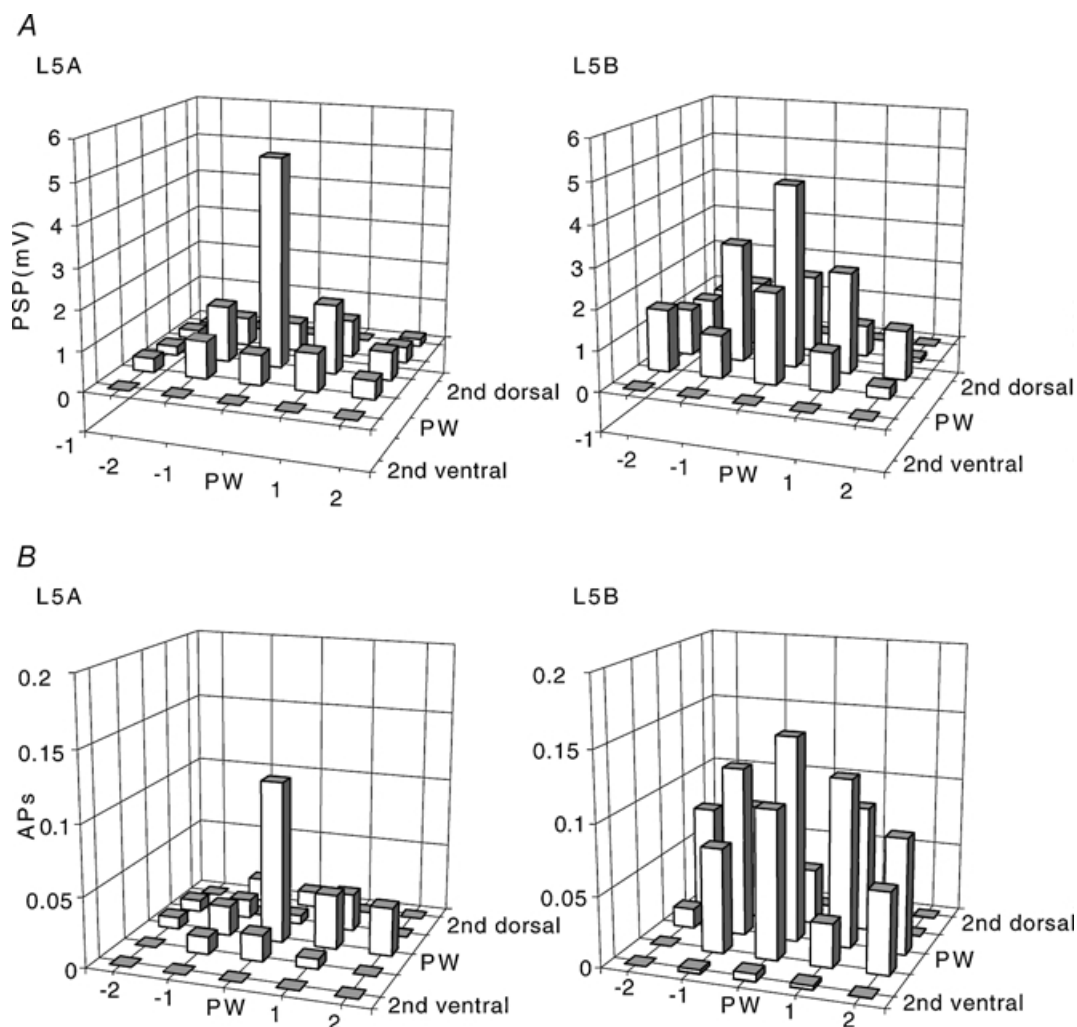

Figure 6. Sub- and suprathreshold receptive fields of layers 5A and 5B somatosensory cells
A, subthreshold averaged RF maps for L5A ($n = 15$) and L5B ($n = 11$) neurones, centred to their principle whisker, with bar height indicating average PSP evoked per whisker deflection. *B*, suprathreshold average RF maps, with bar height indicating average number of spikes evoked (APs) per whisker deflection.

corresponding contralateral responses from representative L5A and L5B cells.

The response to deflections of constant velocity with varying amplitude were studied in a subset of cells ($n = 9$). The reduction of the amplitude to deflection of a PW reduced the response amplitude until the point of response failure. We found no obvious difference between L5A and L5B cells. SuW responses were more sensitive ($n = 4$) to reduction of deflection amplitude; that is, the PW column cells were capable of responding to smaller amplitude stimuli.

Discussion

Our results indicate that the cell bodies of L5A and L5B are preferentially located underneath the walls of barrels in L4, formed by the aggregates of cell bodies of spiny cells. In contrast to L4 cells, basal dendritic and axonal arbors of L5 cells extend across the barrel/column borders defined by the L4 cells. L5 pyramids have, on average, relatively small PW-evoked PSPs but nonetheless more frequently generate APs compared to L2/3 pyramids. L5A has narrow sub- and suprathreshold RFs, with the PW largely
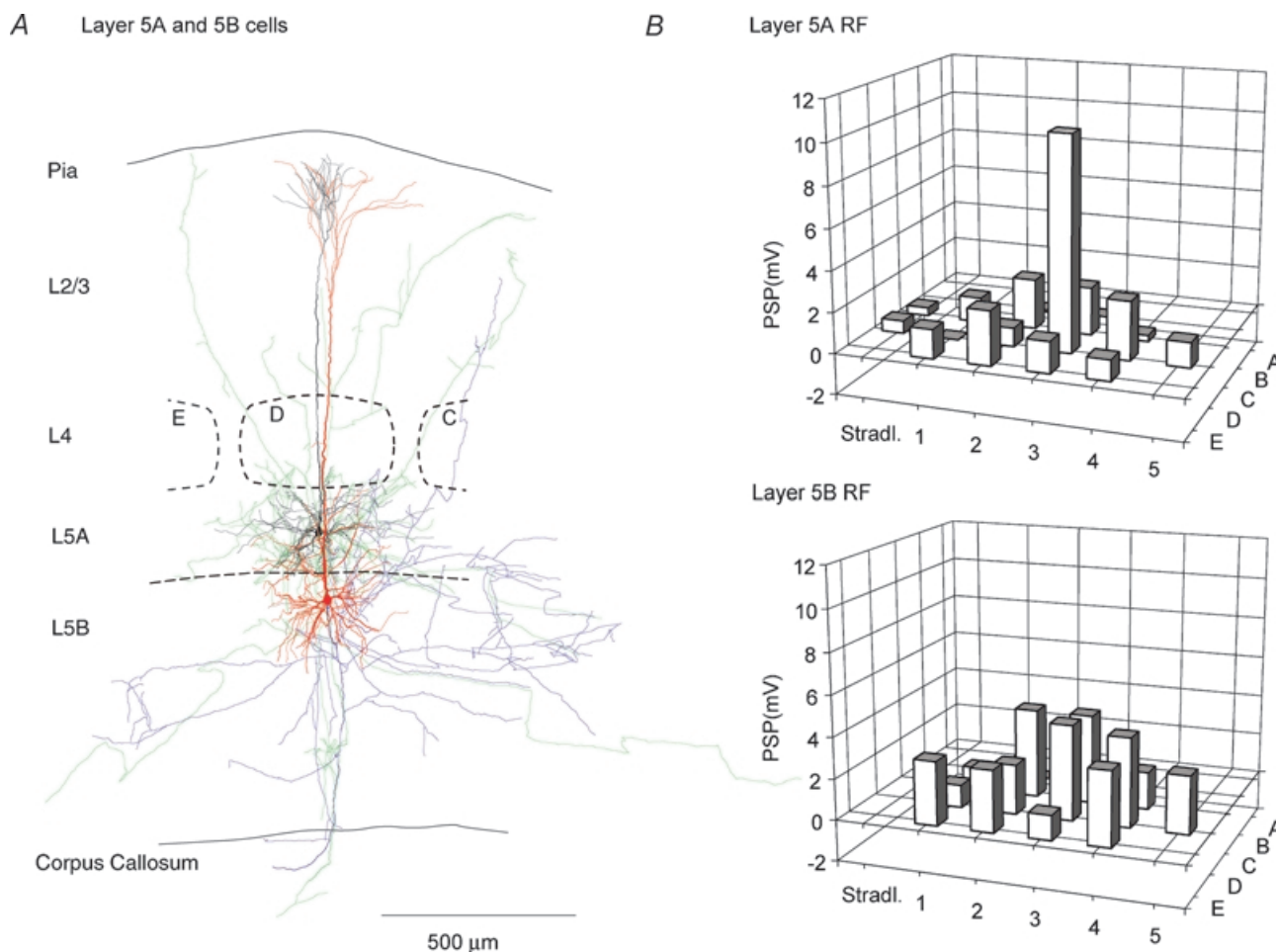

Figure 7. Anatomy and subthreshold receptive fields of a pair of anatomically clustered L5A and L5B somatosensory pyramidal neurones recorded and labelled in succession
A, dendritic (black) and axonal (green) arborizations of the L5A neurone and the dendritic (red) and axonal (blue) arborizations of the L5B neurone are viewed from the coronal perspectives. *B*, subthreshold receptive fields (RFs) for the L5A and L5B cells. The height each bar represents the average postsynaptic potential (PSP) evoked by the stimulation of respective whiskers of the whisker pad (Stradl. refers to the stradler whiskers). D3 whisker stimulation evoked the greatest excitation in both the L5A and the L5B cell.

Table 3. PW PSP characteristics of layer 5 cells

PSP property	PW			Su1W			Su2W		
	All	L5A	L5B	All	L5A	L5B	All	L5A	L5B
Amplitude (mV)	4.9 ± 0.6	5.2 ± 0.8	4.5 ± 0.9	1.6 ± 0.2	1.3 ± 0.3	1.9 ± 0.5	0.6 ± 0.2	0.3 ± 0.1	1.0 ± 0.4
Onset (ms)	10.1 ± 0.5	10.0 ± 0.7	10.3 ± 0.6	11.6 ± 0.4	11.3 ± 0.5	11.9 ± 0.6	13.6 ± 1.5	14.4 ± 2.5	12.6 ± 1.0
Peak (ms)	33.9 ± 3.3	35.1 ± 3.7	32.2 ± 6.2	37.3 ± 2.7	36.5 ± 3.1	38.4 ± 4.8	44.7 ± 6.4	46.9 ± 12.5	42.4 ± 4.4

contributing to a single-column-like excitation whereas the L5B pyramids have broader sub- and suprathreshold RFs, suggesting a multi-column-like excitation in this layer.

Dendrite and axon projection maps, subthreshold RFs and cortical microcircuits

In some cortices RF properties have been considered to acquire complexity in a hierarchal, layer-dependent way, becoming broader in L5 (Kelly & Van Essen, 1974; Simons, 1978; Gilbert & Wiesel, 1979; Armstrong-James *et al.* 1992). From our work in the barrel cortex, this seems not to be the case where RFs of L5 pyramids are narrower than those of L2/3 pyramids. This result raises the question of how the RFs of L5A and L5B cells are constructed by integrating PSPs from thalamocortical and corticocortical afferents. The origin of the different synaptic inputs can possibly be derived from the dimensions of the 2-D maps of dendritic and axonal arbors of L4, L2/3 and L5 cells and by comparing the dynamic structure of L5 RFs (i.e. the latency and the time-dependent amplitude of PW and SuW responses of L5 cells) with that of L4 and L2/3 cells reported previously under the same experimental conditions (Brecht & Sakmann, 2002*a*; Brecht *et al.* 2003).

Innervation of L5A pyramids. Based on previous anatomical work (Koralek *et al.* 1988; Lu & Lin, 1993), firstly a dense projection of axonal arbors from the POm (paralemniscal input) innervates L5A pyramids via the collaterals of axons that innervate the septum cells and septum-related cells in L4 and L2/3, respectively. Secondly, the axonal arbors of identified and reconstructed cortical cells in L4 and L2/3 overlap extensively with the L5A pyramidal cell dendritic domain, suggesting strong innervation by L4 spiny stellate cells (Brecht & Sakmann, 2002*a*; Lübke *et al.* 2003) and L2/3 barrel-related cells (Brecht *et al.* 2003; Lübke *et al.* 2003). In addition, here we document extensive overlap of L5A pyramid dendrites and their axonal arbors within L5A. Thirdly, axonal arbors of L2/3 cells of the ipsilateral barrel cortex overlap with L5

pyramid dendrites from the contralateral cortex (White & DeAmicis, 1977; Olavarria *et al.* 1984; Koralek *et al.* 1990).

The RF of L5A pyramids is highly dynamic (Fig. 9), suggesting that the different inputs will, depending on poststimulus time, contribute differently to the evoked PSP. The onset latency of the PW-evoked PSP is about 10 ms. Afferents that could generate such a rapid initial response are firstly the input from L4 spiny stellate cells excited by single whisker excitation (SWE) cells of the VPM. Secondly some of the POm cells respond rapidly (Ahissar *et al.* 2000) and potentially generate the PSP in septum cells at ~11 ms poststimulus (Brecht & Sakmann, 2002*a*). Collaterals of these cells could contribute to the early PSP in L5A. The later part of the PSP in L5A is most likely generated by the L2/3 and L5A input. The input from L2/3 is probably smaller (Reyes & Sakmann, 1999) than that of the strong L5A intralaminar excitation (Schubert *et al.* 2003). Thirdly the input from contralateral barrel cortex cells may contribute to the late whisker deflection response when both ipsi- and contralateral whiskers are stimulated.

Innervation of L5B pyramids. Anatomical work suggests firstly specific thalamocortical input from the VPM (lemniscal input) to the L5B/L6 boundary (Keller *et al.* 1985; Jensen & Killackey, 1987; Chmielowska *et al.* 1989). Secondly the reconstructions of axonal arbors of identified cells in L4 and L2/3 indicate that a only weak or no overlap exists between L4 axon arbors and L5B dendrites, whereas the axonal arbors of L2/3 cells overlap extensively with L5B (Lübke *et al.* 2003). In addition, input from pyramids within L5B is expected to be strong as 'thick tufted' L5B pyramids are highly interconnected (Markram *et al.* 1997).

The fast onset PSP in L5B pyramids, surprisingly, lags the VPM thalamocortical input to barrel cells in L4 by about 2 ms. One cause for this delay could be that the slow responding multiwhisker excitation cells of the VPM mediate this 10 ms onset PSP (Brecht & Sakmann, 2002*b*). The later PSP components should be generated by L2/3 barrel-related pyramids (Reyes & Sakmann, 1999; Brecht *et al.* 2003) and by L5B pyramids (Markram *et al.* 1997).

Finally when bilateral whisker stimulation occurs as in the case of L5A cells, the ipsilateral whisker is expected to contribute to the late PSP component.

Flow of excitation. Upon deflection of a whisker, two thalamocortical afferent projections are activated, one via the VPM and one via the POm. Both pathways remain, in L4 and L2/3, largely separated (Brecht & Sakmann, 2002*a*; Brecht *et al.* 2003). In L4 and L2/3 the representation of a deflection is 2-fold, the lemniscal RFs being narrower than the paralemniscal RFs. In L5 a deflection is also represented in two ways, focally in L5A and more diffusely in L5B. The dual representation in L5 is clearly the result of the convergence (or merging) of VPM and POm pathways. This convergence is indicated by the fact that the input to L5A from L4 spiny stellate cells is presumably stronger, given the similar narrow L4 and L5A RFs, than that of the POm input, given the dissimilar broad POm and narrow L5A RFs (Diamond *et al.* 1992). The RF of L5B cells is broader than the thalamocortical input from the VPM (Brecht & Sakmann, 2002*b*). This difference reflects, most likely, the broad late L2/3 RFs of barrel-related pyramids
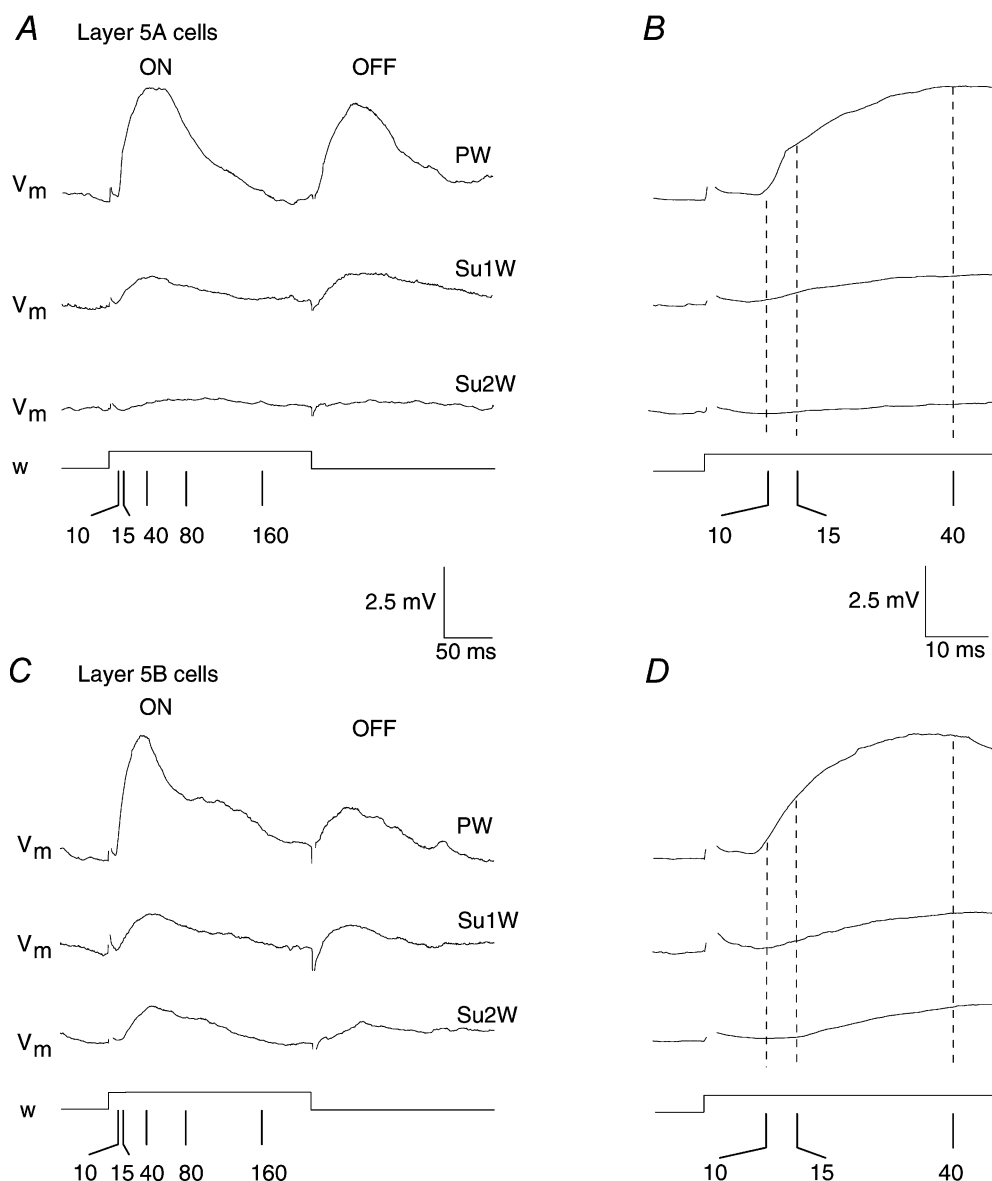

Figure 8. Average membrane potential changes evoked by deflection of principle (PW), primary (Su1W) and secondary (Su2W) surround whiskers
A, average PSPs for L5A neurones (*n* = 16). *B*, onset of L5A responses at higher temporal resolution. *C*, average PSPs for L5B neurones (*n* = 11). *D*, onset of L5B responses at higher temporal resolution.

(Brecht *et al.* 2003) that are likely to contribute to the L5 PSP. Whether and how the paralemniscal inputs (i.e. POm or septum and septum-related cells) contribute to L5B cell RFs is as yet unclear.

Finally one might ask whether and where septum cells and septum-related cell axon arbors converge to form a specific paralemniscal cortical output. Kim & Ebner (1999) noted that selective localization of septal cell terminals in the L5 septal domains were less clear than in those of other layers; although, the axonal arbors of L5 cells located below the septa did show some selective terminal localization in septal domains of the supragranular layers. Moreover, evidence exists for differential corticostriatal projection patterns of L5 neurones located below the barrels and below the septa (Wright *et al.* 2001). Although we recorded no L5 cells below septa, other studies examining layer 5 projection cells have similarly noted that they lie in preferential register with the periphery of the barrels (Crandall *et al.* 1986; Ito, 1992). At present many questions remain about the L5 barrel-related *versus* septum-related functional anatomy. The issue might be resolved by paired

recordings from septum cells in L4 and septum-related cells in L2/3 on the one hand and L5 cells on the other.

Previous work. Both anatomical and electrophysiological studies have placed L5A and L5B within the paralemniscal and lemniscal sensory pathways (Koralek *et al.* 1988; Lu & Lin, 1993; Ahissar *et al.* 2000, 2001). They are thought to represent general and specific sensory information, respectively. Extracellular unit recordings in the vicinity of L5A have described these cells as having very broad RFs (Armstrong-James *et al.* 1992). This discrepancy with our data may be due to a selection bias of unit-recording *versus* whole-cell recording. Broad L5B RFs have been noted both in studies of identified and non-identified neurones (Ito, 1992; Ghazanfar & Nicolelis, 1999). Other studies utilizing whole-cell recordings in the barrel cortex have recorded L5 neurones, but they did not systematically explore the differences between L5A and L5B RFs (Moore & Nelson, 1998; Zhu & Connors, 1999). Some of our results contrast with those of Zhu and Connors, who failed to find
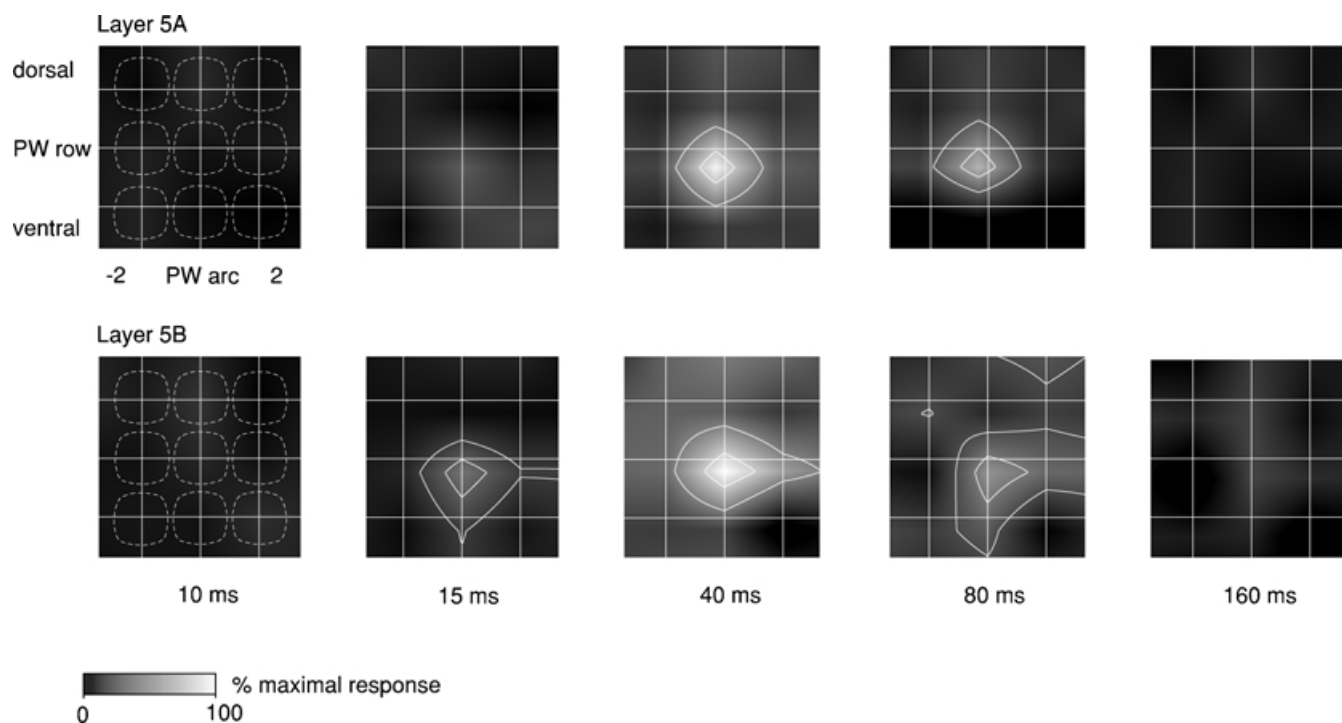

Figure 9. Time dependence of subthreshold RF structure; temporal evolution of the subthreshold responses in L5A and L5B

The grid of white lines indicates the whisker stimulated relative to the PW, in the centre, and the respective barrels, which are superimposed in the 10 ms panel. SuW amplitudes were normalized to the PW PSP maxima. Top and bottom panels show the averaged subthreshold RFs of L5A (*n* = 16) and 5B (*n* = 11) cells, respectively, at different times ranging from 10 to 160 ms following onset of whisker stimulation; note that these are offset to match the area of maximal dendritic L5A and L5B dendritic density from Figs 3*B* and 4*B*. The white lines delineate the areas equal to 80% and 50% of the maximal PW response.
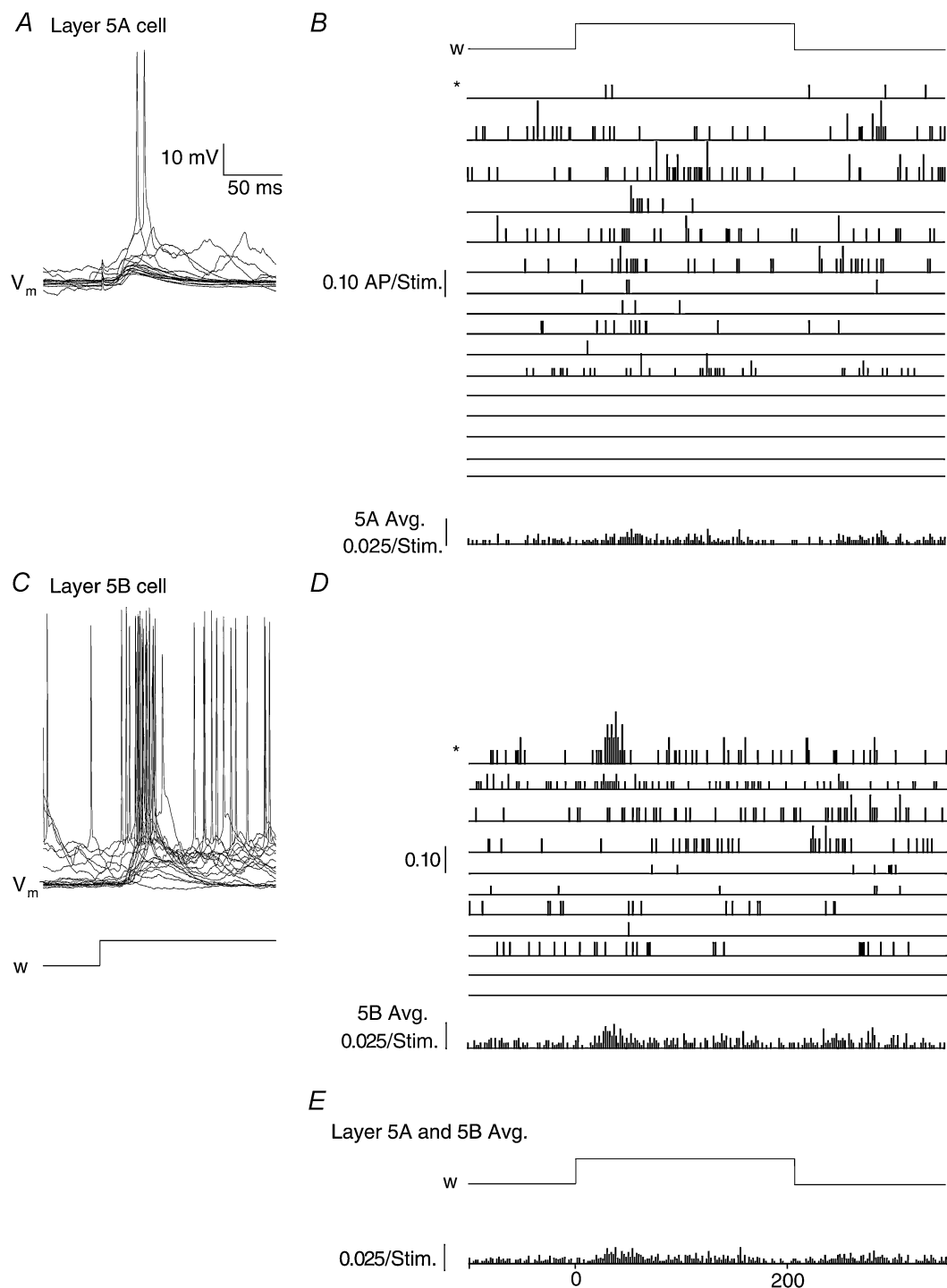
Figure 10. Suprathreshold responses to PW stimulation
A, superimposed traces of responses of a L5A cell to PW deflections show two instances of action potentials. *B*, peristimulus time histograms (PSTHs, bin width 2 ms) for L5A cells over 20 trials, in relation to the principle whisker deflection shown above. The asterix indicates the PSTH of the cell shown in *A*. *C*, superimposed traces of a frequently firing L5B cell in response to whisker stimulation. *D*, PSTHs for L5B cells over 20 trials. The asterix indicates the PSTH of the cell in *C*. *E*, the average PSTH of L5A/L5B whisker-evoked spikes.

any depth- or cell type-specific difference in subthreshold RFs (Zhu & Connors, 1999).

A recent study using whole-cell recordings in visual cortex observed that the stimulus orientation sensitivity of depolarizing responses is increased in L5 cells, so that their subthreshold RF narrows in comparison to those in superficial layers (Martinez *et al.* 2002) in accord with our results.

Functional and anatomical determinants of cortical output from L5

Spontaneous and evoked APs. The spontaneous AP activity of L5 cells (0.5 APs s^{-1}) is higher than that of cells in L4 or L2/3 (0.05 and 0.07 APs s^{-1}, respectively (Brecht & Sakmann, 2002*a*; Brecht *et al.* 2003). This ongoing activity may affect the RFs of such cells. For instance, compared to L5A, L5B cells have a slightly higher rate of spontaneous
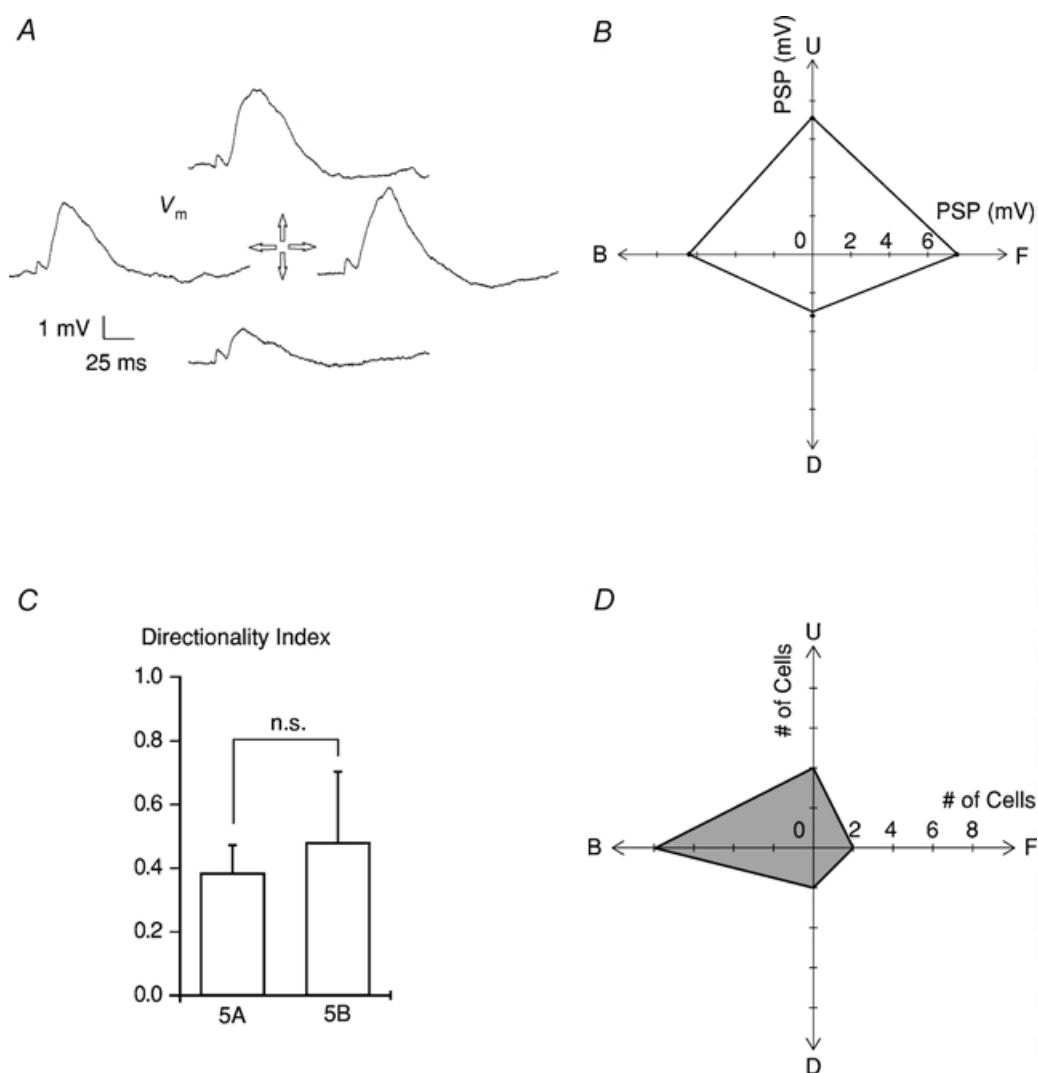

Figure 11. Responses to stimuli of different directions
A, average PSPs of a L5B cell when the PW was deflected in four directions. *B*, the average subthreshold responses of the illustrated cell: backwards (B), forwards (F), upwards (U), and downwards (D). *C*, the directionality index of L5A and L5B cells. Values of 1 would represent completely directional responses, while values of 0 would represent completely non-directional responses. Error bars represent s.e.m. *D*, direction preference of all recorded cells.

firing that may contribute to their larger suprathreshold *versus* subthreshold RF. Spontaneous AP activity occurs during the up-state, and whisker-evoked AP responses vary due to the ongoing subthreshold up- and down-state activity (Sachdev & Wilson, 2001; Petersen *et al.* 2003). This variation will influence the suprathreshold RFs. Extracellular recordings also indicate that L5 cells have higher spontaneous AP activity than other layers (Armstrong-James & Fox, 1987; Huang *et al.* 1998). These
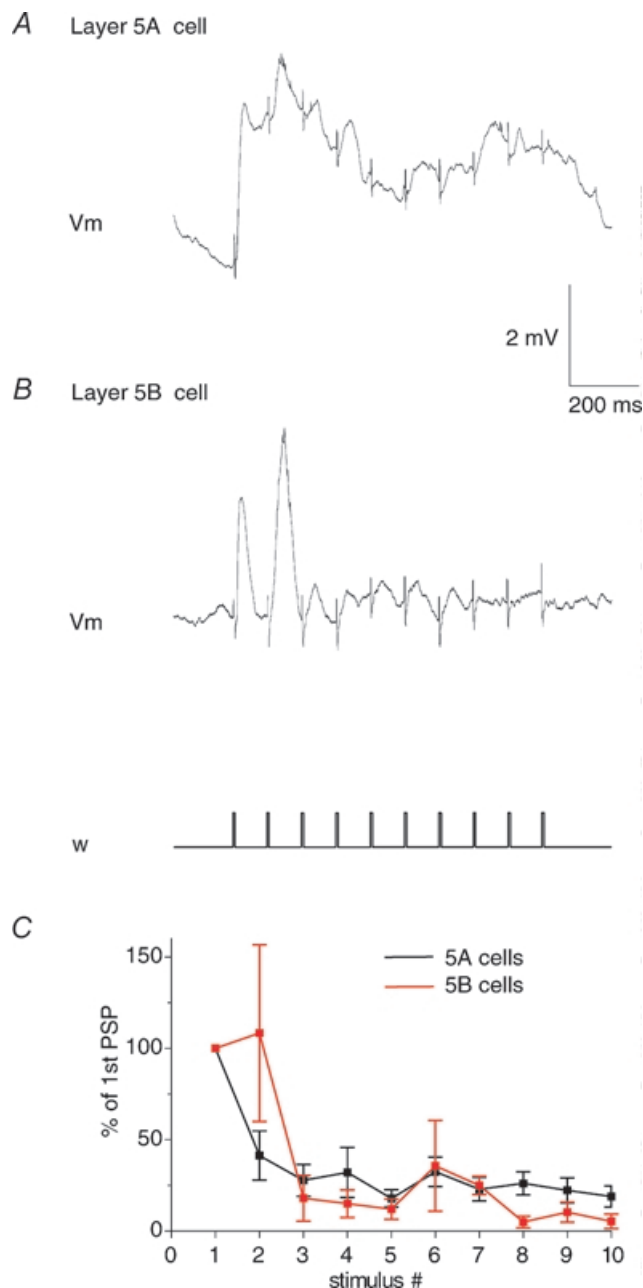
findings together suggest that L5 is a major constituent of ongoing cortical output activity. This is probably due to a collection of factors. The first may be the relatively depolarized resting membrane potential of the L5 cells, on average ~10 mV more depolarized than that of L4 and L2/3 neurones (Brecht & Sakmann, 2002*a*; Brecht *et al.* 2003). Since they rest relatively close to AP threshold, they will tend to fire more often and can be fired by smaller PSPs. This combined with L5 recurrent excitation via the intralaminar connections (Figs 3 and 4) (Chagnac-Amitai *et al.* 1990; Markram, 1997; Markram *et al.* 1997) may act to boost the rate of both ongoing and evoked APs.

The average L5 PW PSP is only about 5 mV, while unitary connections arising from other L5 and L2/3 cells are ~0.3 and ~0.1 mV, respectively (Reyes & Sakmann, 1999). Since these cells are thought to receive approximately 5000–15 000 synapses (Larkman, 1991), L5 responses should be assembled from relatively few presynaptic cells, indicating sparse presynaptic activity, as has been postulated for the PSP responses in L4 and L2/3 neurones (Brecht & Sakmann, 2002*a*; Brecht *et al.* 2003).

Cortical barrels and modules. An anatomical organizing principle of sensory cortices is the modules of L5 pyramids, often in combination with L2/3 pyramids (White & Peters,
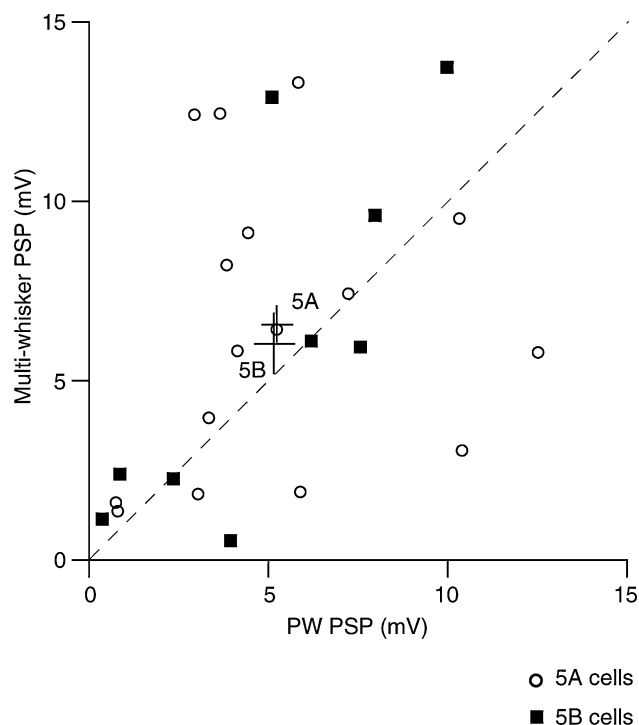

Figure 12. Responses to repetitive PW stimulation
Stimuli were brief deflections applied at 10 Hz. *A*, average response of L5A cells. *B*, average response of L5B cells. *C*, average percentage of subsequent responses (± S.E.M.) compared to first response amplitude.

Figure 13. Responses to single and multi-whisker stimulation
Plot of multi-whisker response amplitude *versus* PW response amplitudes for L5A and L5B cells. The two bars indicate the means ± S.E.M.

1993). In the barrel cortex the somata of L5 pyramids are preferentially located underneath the somata of the L4 spiny cells that form the barrels. The dendrites and axons of L4 cells are orientated towards the barrel hollows and respect the borders of barrels whereas the dendrites of L5 cells extend well across borders of barrel-columns. Thus the barrel-column organization in L4 and L2/3 is replaced in L5 by an organization of smaller, more frequent modules. Functionally these modules convey the signals of a single or a few barrel columns with which they are associated.

Number of APs per deflection. How many L5 axons carry the AP output signalling that a whisker deflection has occurred? The distance between apical dendrite clusters of L5 cells forming modules is about 50 μm (White & Peters, 1993). Thus single-column-like excitation of L5 cells would mean that ~100 cortical modules can be activated by a deflection. Each module comprises about 20–50 L5 cells, implying that they represent ~2000–5000 L5 cells in a column (White & Peters, 1993). Although only about half of the cells increased their firing with a deflection, the average number of APs per stimulus in L5 cells is close to 0.1. Otherwise stated, on average 10% of cells will fire an AP on any given stimulus. As such, the AP output is conveyed by about 200–500 pyramids of L5; meaning that, on average, 2–5 APs per module originate from L5 cells signalling that a deflection has occurred.

Output from the barrel cortex is also mediated by APs in L2/3 pyramids, which in primary sensory areas co-cluster with L5 cells (White & Peters, 1993). The number of APs in L2/3 pyramids of a barrel-column has been estimated to be about 120 (Brecht *et al.* 2003). If the L2/3 cells contribute to the modules' output, a total of ~300–600 APs per deflection are conveyed out of the barrel cortex. On average then, the number of APs generated in a module might exceed 5.

Bilateral representation. Recent work has implicated L5 in mediating discrimination of bilateral stimuli (Shuler *et al.* 2001, 2002). Our results indicate that both L5A and L5B cells receive a relatively small and longer-onset latency ipsilateral whisker input, while both L4 and L2/3 appear devoid of such input (Brecht & Sakmann, 2002*a*; Brecht *et al.* 2003). Such bilateral sensory representation presents an additional important example of how sensory signals are integrated by the cortex (Berlucchi *et al.* 1967; Hubel & Wiesel, 1967; Iwamura, 2000).

Functional significance

How the PW-specific L5A output will affect its target cells in other cortical areas and in subcortical nuclei is as

yet unclear. Whisker stimulation evokes short-latency APs in motor cortex neurones dependent on somatosensory cortex afferents (Farkas *et al.* 1999), which may originate in part from L5A neurones (Koralek *et al.* 1990). Similarly, L5A whisker-specific input would signal to the secondary somatosensory cortex (S2) in decision-making processes related to stimulus properties (Romo *et al.* 2002). In addition it may influence movement preparation encoded by the caudate nucleus in response to sensory stimuli (Mercier *et al.* 1990; Romo & Schultz, 1992; Schultz & Romo, 1992). Behavioural experiments have recently shown that L5A has the lowest electrical stimulation thresholds for evoking motor responses (Krauss *et al.* 2003), emphasizing the importance of the downstream effects of L5A's intracortical and subcortical projections in generating behavioural responses.
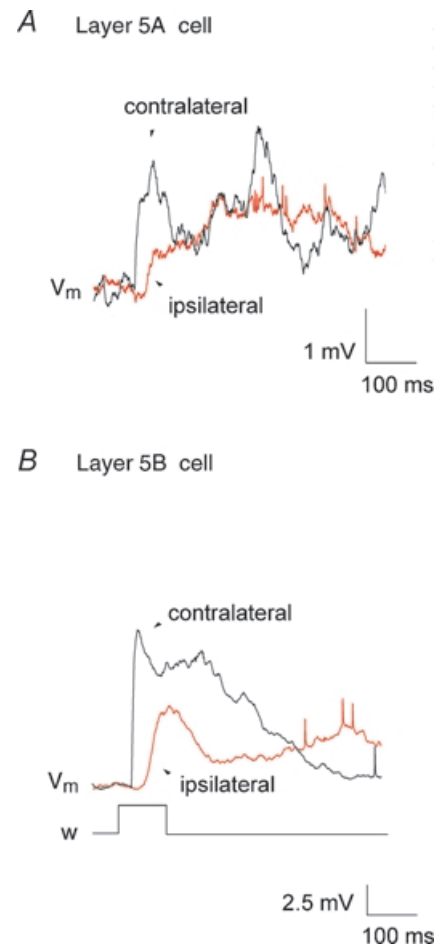

Figure 14. Responses to contralateral *versus* ispilateral multi-whisker stimulation
Average membrane potential changes evoked in a L5A and a L5B cell by multi-whisker airpuff stimuli delivered to contralateral and ipsilateral whiskers.

L5B output could increase the excitation for whisker-directed behaviours in areas receiving whisker-specific information directly from different parts of the trigeminal nucleus, such as the pontine nuclei, superior colliculus and the facial nucleus (Killackey & Erzurumlu, 1981; Swenson *et al.* 1984; Rhoades *et al.* 1989; Dauvergne *et al.* 2001, 2002).

Conclusions

Our description of the dynamic sub- and suprathreshold RFs of cortical neurones in L4 and L2/3 (Brecht & Sakmann, 2002*a*; Brecht *et al.* 2003), in combination with the RFs reported here for pyramids in L5, suggest that in each layer of the barrel cortex a whisker deflection is represented in at least two ways by anatomically segregated ensembles of neurones. In L4, the cortical *recipient* layer, the thalamocortical inputs segregate into barrel cells, representing focal excitation, and septum cells, representing more diffuse excitation. This segregation is maintained in L2/3. In L5, the cortical *output* layer, a deflection is represented by focal excitation in L5A and more diffuse excitation in L5B. The 2-D projection maps of dendritic and axonal arbors of identified cells in granular, supra- and infragranular layers indicate a mixing of the two afferent pathways at the level of L5. How exactly the dual representation in L5 is established, i.e. what are the most efficacious inputs, remains to be elucidated by paired recordings from different presynaptic cells targeting L5A or L5B cells and determining their unitary EPSPs.

Finally it is yet to be elucidated whether the behaviourally relevant cortical output of L5 is 'layer specific' or 'module specific'. A layer specific patterning of output effects has recently been demonstrated in the rat vibrissa motor cortex (Brecht *et al.* 2004). In barrel cortex it remains to be determined whether stimulus properties are signalled independently either by cells in L5A or cells in L5B, or whether it is the pattern of APs in L5A and L5B across an ensemble of modules that is relevant for initiating behavioural responses.

References

Ahissar E, Sosnik R, Bagdasarian K & Haidarliu S (2001). Temporal frequency of whisker movement. II. Laminar organization of cortical representations. *J Neurophysiol* **86**, 354–367.

Ahissar E, Sosnik R & Haidarliu S (2000). Transformation from temporal to rate coding in a somatosensory thalamocortical pathway. *Nature* **406**, 302–306.

Anderson J, Lampl I, Reichova I, Carandini M & Ferster D (2000). Stimulus dependence of two-state fluctuations of membrane potential in cat visual cortex. *Nat Neurosci* **3**, 617–621.

Armstrong-James M & Fox K (1987). Spatiotemporal convergence and divergence in the rat S1 'barrel' cortex. *J Comp Neurol* **263**, 265–281.

Armstrong-James M, Fox K & Das-Gupta A (1992). Flow of excitation within rat barrel cortex on striking a single vibrissa. *J Neurophysiol* **68**, 1345–1358.

Berlucchi G, Gazzaniga MS & Rizzolatti G (1967). Microelectrode analysis of transfer of visual information by the corpus callosum. *Arch Ital Biol* **105**, 583–596.

Bernardo KL, McCasland JS & Woolsey TA (1990*a*). Local axonal trajectories in mouse barrel cortex. *Exp Brain Res* **82**, 247–253.

Bernardo KL, McCasland JS, Woolsey TA & Strominger RN (1990*b*). Local intra- and interlaminar connections in mouse barrel cortex. *J Comp Neurol* **291**, 231–255.

Blanton MG, Lo Turco JJ & Kriegstein AR (1989). Whole cell recording from neurons in slices of reptilian and mammalian cerebral cortex. *J Neurosci Meth* **30**, 203–210.

Brecht M, Roth A & Sakmann B (2003). Dynamic receptive fields of reconstructed pyramidal cells in layers 3 and 2 of the rat somatosensory cortex. *J Physiol*, **553**, 243–265.

Brecht M & Sakmann B (2002*a*). Dynamic representation of whisker deflection by synaptic potentials in spiny stellate and pyramidal cells in the barrels and septa of layer 4 rat somatosensory cortex. *J Physiol* **543**, 49–70.

Brecht M & Sakmann B (2002*b*). Whisker maps of neuronal subclasses of the rat ventral posterior medial thalamus, identified by whole-cell voltage recording and morphological reconstruction. *J Physiol* **538**, 495–515.

Brecht M, Schneider M, Sakmann B & Margrie T (2004). Whisker movements evoked by stimulation of single pyramidal cells in rat motor cortex. *Nature* **427**, 704–710.

Chagnac-Amitai Y, Luhmann HJ & Prince DA (1990). Burst generating and regular spiking layer 5 pyramidal neurons of rat neocortex have different morphological features. *J Comp Neurol* **296**, 598–613.

Chmielowska J, Carvell GE & Simons DJ (1989). Spatial organization of thalamocortical and corticothalamic projection systems in the rat SmI barrel cortex. *J Comp Neurol* **285**, 325–338.

Cowan RL & Wilson CJ (1994). Spontaneous firing patterns and axonal projections of single corticostriatal neurons in the rat medial agranular cortex. *J Neurophysiol* **71**, 17–32.

Crandall JE, Korde M & Caviness VS Jr (1986). Somata of layer V projection neurons in the mouse barrelfield cortex are in preferential register with the sides and septa of the barrels. *Neurosci Lett* **67**, 19–24.

Dauvergne C, Pinganaud G, Buisseret P, Buisseret-Delmas C & Zerari-Mailly F (2001). Reticular premotor neurons projecting to both facial and hypoglossal nuclei receive trigeminal afferents in rats. *Neurosci Lett* **311**, 109–112.

Dauvergne C, Zerari-Mailly F, Buisseret P, Buisseret-Delmas C & Pinganaud G (2002). The sensory trigeminal complex projects contralaterally to the facial motor and the accessory abducens nuclei in the rat. *Neurosci Lett* **329**, 169–172.

Deschenes M, Bourassa J & Pinault D (1994). Corticothalamic projections from layer V cells in rat are collaterals of long-range corticofugal axons. *Brain Res* **664**, 215–219.

Diamond ME, Armstrong-James M & Ebner FF (1992). Somatic sensory responses in the rostral sector of the posterior group (POm) and in the ventral posterior medial nucleus (VPM) of the rat thalamus. *J Comp Neurol* **318**, 462–476.

Farkas T, Kis Z, Toldi J & Wolff JR (1999). Activation of the primary motor cortex by somatosensory stimulation in adult rats is mediated mainly by associational connections from the somatosensory cortex. *Neuroscience* **90**, 353–361.

Feldman ML & Peters A (1974). A study of barrels and pyramidal dendritic clusters in the cerebral cortex. *Brain Res* **77**, 55–76.

Friedberg MH, Lee SM & Ebner FF (1999). Modulation of receptive field properties of thalamic somatosensory neurons by the depth of anesthesia. *J Neurophysiol* **81**, 2243–2252.

Ghazanfar AA & Nicolelis MA (1999). Spatiotemporal properties of layer V neurons of the rat primary somatosensory cortex. *Cereb Cortex* **9**, 348–361.

Gilbert CD & Wiesel TN (1979). Morphology and intracortical projections of functionally characterised neurones in the cat visual cortex. *Nature* **280**, 120–125.

Gottlieb JP & Keller A (1997). Intrinsic circuitry and physiological properties of pyramidal neurons in rat barrel cortex. *Exp Brain Res* **115**, 47–60.

Hoeflinger BF, Bennett-Clarke CA, Chiaia NL, Killackey HP & Rhoades RW (1995). Patterning of local intracortical projections within the vibrissae representation of rat primary somatosensory cortex. *J Comp Neurol* **354**, 551–563.

Horikawa K & Armstrong WE (1988). A versatile means of intracellular labeling: injection of biocytin and its detection with avidin conjugates. *J Neurosci Meth* **25**, 1–11.

Huang W, Armstrong-James M, Rema V, Diamond ME & Ebner FF (1998). Contribution of supragranular layers to sensory processing and plasticity in adult rat barrel cortex. *J Neurophysiol* **80**, 3261–3271.

Hubel DH & Wiesel TN (1967). Cortical and callosal connections concerned with the vertical meridian of visual fields in the cat. *J Neurophysiol* **30**, 1561–1573.

Ito M (1981). Some quantitative aspects of vibrissa-driven neuronal responses in rat neocortex. *J Neurophysiol* **46**, 705–715.

Ito M (1992). Simultaneous visualization of cortical barrels and horseradish peroxidase-injected layer 5b vibrissa neurones in the rat. *J Physiol* **454**, 247–265.

Iwamura Y (2000). Bilateral receptive field neurons and callosal connections in the somatosensory cortex. *Philos Trans R Soc Lond B Biol Sci* **355**, 267–273.

Jensen KF & Killackey HP (1987). Terminal arbors of axons projecting to the somatosensory cortex of the adult rat. I. The normal morphology of specific thalamocortical afferents. *J Neurosci* **7**, 3529–3543.

Keller A, White EL & Cipolloni PB (1985). The identification of thalamocortical axon terminals in barrels of mouse SmI cortex using immunohistochemistry of anterogradely transported lectin (Phaseolus vulgaris-leucoagglutinin). *Brain Res* **343**, 159–165.

Kelly JP & Van Essen DC (1974). Cell structure and function in the visual cortex of the cat. *J Physiol* **238**, 515–547.

Killackey H & Ebner F (1973). Convergent projection of three separate thalamic nuclei on to a single cortical area. *Science* **179**, 283–285.

Killackey HP & Erzurumlu RS (1981). Trigeminal projections to the superior colliculus of the rat. *J Comp Neurol* **201**, 221–242.

Killackey HP, Koralek KA, Chiaia NL & Rhodes RW (1989). Laminar and areal differences in the origin of the subcortical projection neurons of the rat somatosensory cortex. *J Comp Neurol* **282**, 428–445.

Kim U & Ebner FF (1999). Barrels and septa: separate circuits in rat barrels field cortex. *J Comp Neurol* **408**, 489–505.

Koralek KA, Jensen KF & Killackey HP (1988). Evidence for two complementary patterns of thalamic input to the rat somatosensory cortex. *Brain Res* **463**, 346–351.

Koralek KA, Olavarria J & Killackey HP (1990). Areal and laminar organization of corticocortical projections in the rat somatosensory cortex. *J Comp Neurol* **299**, 133–150.

Krauss A, Manns ID & Brecht M (2003). Lamniar distribution of detection thresholds for electric stimulation in rat barrel cortex. In *Abstracts Society for Neuroscience*. New Orleans. Program no. 58. 19.2003.

Larkman AU (1991). Dendritic morphology of pyramidal neurones of the visual cortex of the rat. III. Spine distributions. *J Comp Neurol* **306**, 332–343.

Larkum ME & Zhu JJ (2002). Signaling of layer 1 and whisker-evoked Ca^{2+} and Na^{+} action potentials in distal and terminal dendrites of rat neocortical pyramidal neurons *in vitro* and *in vivo*. *J Neurosci* **22**, 6991–7005.

Larkum ME, Zhu JJ & Sakmann B (1999). A new cellular mechanism for coupling inputs arriving at different cortical layers. *Nature* **398**, 338–341.

Lev DL & White EL (1997). Organization of pyramidal cell apical dendrites and composition of dendritic clusters in the mouse: emphasis on primary motor cortex. *Eur J Neurosci* **9**, 280–290.

Lu SM & Lin RC (1993). Thalamic afferents of the rat barrel cortex: a light- and electron- microscopic study using Phaseolus vulgaris leucoagglutinin as an anterograde tracer. *Somatosens Mot Res* **10**, 1–16.

Lübke J, Roth A, Feldmeyer D & Sakmann B (2003). Morphometric analysis of the columnar innervation domain of neurons connecting layer 4 and layer 2/3 of juvenile rat barrel cortex. *Cereb Cortex* **13**, 1051–1063.

Margrie TW, Brecht M & Sakmann B (2002). *In vivo*, low-resistance, whole-cell recordings from neurons in the anaesthetized and awake mammalian brain. *Pflugers Arch* **444**, 491–498.

Markram H (1997). A network of tufted layer 5 pyramidal neurons. *Cereb Cortex* **7**, 523–533.

Markram H, Lübke J, Frotscher M, Roth A & Sakmann B (1997). Physiology and anatomy of synaptic connections between thick tufted pyramidal neurones in the developing rat neocortex. *J Physiol* **500**, 409–440.

Martinez LM, Alonso JM, Reid RC & Hirsch JA (2002). Laminar processing of stimulus orientation in cat visual cortex. *J Physiol* **540**, 321–333.

Mercier BE, Legg CR & Glickstein M (1990). Basal ganglia and cerebellum receive different somatosensory information in rats. *Proc Natl Acad Sci U S A* **87**, 4388–4392.

Moore CI & Nelson SB (1998). Spatio-temporal subthreshold receptive fields in the vibrissa representation of rat primary somatosensory cortex. *J Neurophysiol* **80**, 2882–2892.

Olavarria J, Van Sluyters RC & Killackey HP (1984). Evidence for the complementary organization of callosal and thalamic connections within rat somatosensory cortex. *Brain Res* **291**, 364–368.

Petersen CC, Hahn TT, Mehta M, Grinvald A & Sakmann B (2003). Interaction of sensory responses with spontaneous depolarization in layer 2/3 barrel cortex. *Proc Natl Acad Sci U S A* **100**, 13638–13643.

Reyes A & Sakmann B (1999). Developmental switch in the short-term modification of unitary EPSPs evoked in layer 2/3 and layer 5 pyramidal neurons of rat neocortex. *J Neurosci* **19**, 3827–3835.

Rhoades RW, Fish SE, Chiaia NL, Bennett-Clarke C & Mooney RD (1989). Organization of the projections from the trigeminal brainstem complex to the superior colliculus in the rat and hamster: anterograde tracing with Phaseolus vulgaris leucoagglutinin and intra-axonal injection. *J Comp Neurol* **289**, 641–656.

Romo R, Hernandez A, Zainos A, Lemus L & Brody CD (2002). Neuronal correlates of decision-making in secondary somatosensory cortex. *Nat Neurosci* **5**, 1217–1225.

Romo R & Schultz W (1992). Role of primate basal ganglia and frontal cortex in the internal generation of movements. III. Neuronal activity in the supplementary motor area. *Exp Brain Res* **91**, 396–407.

Sachdev RN & Wilson CJ (2001). Mechanisms underlying the trial to trial variability in response to whisker stimulation in rat barrel cortex. *Soc Neurosci Abstr* **393**, 17.2001.

Schubert D, Kotter R, Zilles K, Luhmann HJ & Staiger JF (2003). Functional input connectivity of layer VA pyramidal cells in rat barrel cortex. Sixth IBRO World Congress of Neuroscience, p. 424. Prague.

Schultz W & Romo R (1992). Role of primate basal ganglia and frontal cortex in the internal generation of movements. I. Preparatory activity in the anterior striatum. *Exp Brain Res* **91**, 363–384.

Shuler MG, Krupa DJ & Nicolelis MA (2001). Bilateral integration of whisker information in the primary somatosensory cortex of rats. *J Neurosci* **21**, 5251–5261.

Shuler MG, Krupa DJ & Nicolelis MA (2002). Integration of bilateral whisker stimuli in rats: role of the whisker barrel cortices. *Cereb Cortex* **12**, 86–97.

Simons DJ (1978). Response properties of vibrissa units in rat SI somatosensory neocortex. *J Neurophysiol* **41**, 798–820.

Simons DJ (1983). Multi-whisker stimulation and its effects on vibrissa units in rat SmI barrel cortex. *Brain Res* **276**, 178–182.

Swenson RS, Kosinski RJ & Castro AJ (1984). Topography of spinal, dorsal column nuclear, and spinal trigeminal projections to the pontine gray in rats. *J Comp Neurol* **222**, 301–311.

Veinante P, Lavallee P & Deschenes M (2000). Corticothalamic projections from layer 5 of the vibrissal barrel cortex in the rat. *J Comp Neurol* **424**, 197–204.

White EL & DeAmicis RA (1977). Afferent and efferent projections of the region in mouse SmL cortex which contains the posteromedial barrel subfield. *J Comp Neurol* **175**, 455–482.

White EL & Peters A (1993). Cortical modules in the posteromedial barrel subfield (Sml) of the mouse. *J Comp Neurol* **334**, 86–96.

Wise SP & Jones EG (1977). Cells of origin and terminal distribution of descending projections of the rat somatic sensory cortex. *J Comp Neurol* **175**, 129–157.

Wong-Riley M (1979). Changes in the visual system of monocularly sutured or enucleated cats demonstrable with cytochrome oxidase histochemistry. *Brain Res* **171**, 11–28.

Woolsey TA & Van der Loos H (1970). The structural organization of layer IV in the somatosensory region (SI) of mouse cerebral cortex. The description of a cortical field composed of discrete cytoarchitectonic units. *Brain Res* **17**, 205–242.

Wright AK, Ramanathan S & Arbuthnott GW (2001). Identification of the source of the bilateral projection system from cortex to somatosensory neostriatum and an exploration of its physiological actions. *Neuroscience* **103**, 87–96.

Zhu JJ & Connors BW (1999). Intrinsic firing patterns and whisker-evoked synaptic responses of neurons in the rat barrel cortex. *J Neurophysiol* **81**, 1171–1183.

Acknowledgements